

ANALYSIS OF A FULLY DISCRETE APPROXIMATION FOR THE CLASSIC KELLER-SEGEL MODEL: LOWER AND *A PRIORI* BOUNDS

JUAN VICENTE GUTIÉRREZ-SANTACREU[†] AND JOSÉ RAFAEL RODRÍGUEZ-GALVÁN[‡]

ABSTRACT. This paper is devoted to constructing approximate solutions for the classical Keller–Segel model governing *chemotaxis*. It consists of a system of nonlinear parabolic equations, where the unknowns are the average density of cells (or organisms), which is a conserved variable, and the average density of chemoattractant.

The numerical proposal is made up of a crude finite element method together with a mass lumping technique and a semi-implicit Euler time integration. The resulting scheme turns out to be linear and decouples the computation of variables. The approximate solutions keep lower bounds – positivity for the cell density and nonnegativity for the chemoattractant density –, are bounded in the $L^1(\Omega)$ -norm, satisfy a discrete energy law, and have *a priori* energy estimates. The latter is achieved by means of a discrete Moser–Trudinger inequality. As far as we know, our numerical method is the first one that can be encountered in the literature dealing with all of the previously mentioned properties at the same time. Furthermore, some numerical examples are carried out to support and complement the theoretical results.

2010 Mathematics Subject Classification. 35K20, 35K55, 65K60.

Keywords. Keller–Segel equations; non-linear parabolic equations; finite-element approximation; lower bounds; *a priori* bounds.

CONTENTS

1. Introduction	2
1.1. Aims	2
1.2. The Keller–Segel equations	2
1.3. Notation	3
1.4. Outline	4
2. Technical preliminaries	4
2.1. Hypotheses	4
2.2. Auxiliary results	4
3. Presentation of main result	7
4. Proof of main result	9
4.1. Lower bounds and a discrete energy law	9
4.2. <i>A priori</i> bounds	13
4.3. Induction argument	17
5. Computational experiments	19
5.1. Non-blowup setting	19
5.2. Blowup setting	21
References	23

Date: September 23, 2020.

JVGS and JRRG were partially supported by the Spanish Grant No. PGC2018-098308-B-I00 from Ministerio de Ciencias e Innovación - Agencia Estatal de Investigación with the participation of FEDER.

1. INTRODUCTION

1.1. Aims. In 1970/71 Keller and Segel [17, 18] attempted to derive a set of equations for modeling *chemotaxis* – a biological process through which an organism (or a cell) migrates in response to a chemical stimulus being attractant or repellent. It is nowadays well-known that the work of Keller and Segel turned out to be somehow biologically inaccurate since their equations provide unrealistic solutions; a little more precisely, solutions that blow up in finite time. Such a phenomenon does not occur in nature. Even though the original Keller–Segel equations are less relevant from a biological point of view, they are mathematically of great interest.

Much of work for the Keller–Segel equations has been carried out in developing purely analytical results, whereas there are very few numerical results in the literature. This is due to the fact that solving numerically the Keller–Segel equations is a challenging task because their solutions exhibit many interesting mathematical properties which are not easily adapted to a discrete framework. For instance, solutions to the Keller–Segel equations satisfy lower bounds (positivity and non-negativity) and enjoy an energy law, which is obtained by testing the equations against non linear functions. Cross-diffusion mechanisms governing the chemotactic phenomena are the responsible for the Keller–Segel equations to be so difficult not only theoretically but also numerically.

In spite of being a limited model, it is hoped that developing and analyzing numerical methods for the classical Keller–Segel equations may open new roads to deeper insights and better understandings for dealing with the numerical approximation of other chemotaxis models – biologically more realistic –, but which are, however, inspired on the original Keller–Segel formulation. In a nutshell, these other chemotaxis models are modifications of the Keller–Segel equations in order to avoid the non-physical blow up of solutions and hence produce solutions being closer to chemotaxis phenomena. For these other chemotaxis models, it is recommended the excellent surveys of Hillen and Painter [13], Horstmann [14, 15], and, more recently, Bellomo, Bellouquid, Tao, and Winkler [1]. In these surveys the authors reviewed to date as to when they were written the state of art of modeling and mathematical analysis for the Keller–Segel equations and their variants.

It is our aim in this work to design a fully discrete algorithm for the classical Keller–Segel equations based on a finite element discretization whose discrete solutions satisfy lower and *a priori* bounds.

1.2. The Keller–Segel equations. Let $\Omega \subset \mathbb{R}^2$ be a bounded domain, with \mathbf{n} being its outward-directed unit normal vector to Ω , and let $[0, T]$ be a time interval. Take $Q = (0, T] \times \Omega$ and $\Sigma = (0, T] \times \partial\Omega$. Then the boundary-value problem for the Keller–Segel equations reads as follows. Find $u : \bar{Q} \rightarrow (0, \infty)$ and $v : \bar{Q} \rightarrow [0, \infty)$ satisfying

$$(1) \quad \begin{cases} \partial_t u - \Delta u &= -\nabla \cdot (u \nabla v) & \text{in } Q, \\ \partial_t v - \Delta v &= u - v & \text{in } Q, \end{cases}$$

subject to the initial conditions

$$(2) \quad u(0) = u_0 \quad \text{and} \quad v(0) = v_0 \quad \text{in } \Omega,$$

and the boundary conditions

$$(3) \quad \nabla u \cdot \mathbf{n} = 0 \quad \text{and} \quad \nabla v \cdot \mathbf{n} = 0 \quad \text{on } \Sigma.$$

Here u is the average density of organisms (or cells), which is a conserved variable, and v is the average density of chemical sign, which is a nonconserved variable.

System (1) was motivated by Keller and Segel [17] describing the aggregation phenomena exhibited by the amoeba *Dictyostelium discoideum* due to an attractive chemical substance referred to as *chemoattractant*, which is generated by the own amoeba and is, nevertheless, degraded by living conditions. Moreover, diffusion is also presented in the motion of amoebae and chemoattractant.

The diffusion phenomena performed by cells and chemoattractant are modelled by the terms $-\Delta u$ and $-\Delta v$, respectively, whereas the aggregation mechanism is described by the term $-\nabla \cdot (u \nabla v)$. It is this nonlinear term that is the major difficulty in studying system (1). Further the production and degradation of chemoattractant are associated with the term $u - v$.

Concerning the mathematical analysis for system (1), Nagai, Senba, and Yoshida [19] proved existence, uniqueness and regularity of solutions under the condition $\int_{\Omega} u_0(\mathbf{x}) d\mathbf{x} \in (0, 4\pi)$. In proving this, a variant of Moser–Trdinguer’s inequality was used. In the particular case that Ω be a ball, the above-mentioned condition becomes $\int_{\Omega} u_0(\mathbf{x}) d\mathbf{x} \in (0, 8\pi)$. Herrero and Velázquez [12] dealt with the first blow-up framework by constructing some radially symmetric two-dimensional solutions which blow up within finite time. The next progress in this sense with Ω being non-radial and simply connected was the work of Horstmann and Wang [16] who found some unbounded solutions provided that $\int_{\Omega} u_0(\mathbf{x}) d\mathbf{x} > 4\pi$ and $\int_{\Omega} u_0(\mathbf{x}) d\mathbf{x} \notin \{4k\pi \mid k \in \mathbb{N}\}$. So far there is no supporting evidence as to whether such solutions may evolve to produce a blow-up phenomenon within finite time or whether, on the contrary, may increase to infinity with time. In three dimensions, Winkler [24] proved that there exist radially symmetric solutions blowing up in finite time for any value of $\int_{\Omega} u_0(\mathbf{x}) d\mathbf{x}$.

The main tool [24] in proving blow-up solutions is the energy law which stems from system (1). Nevertheless, an inadequate approximation of lower bounds can trigger off oscillations of the variables, which can lead to spurious, blow-up solutions.

Concerning the numerical analysis for system (1), very little is said about numerical algorithms which keep lower bounds, are $L^1(\Omega)$ -bounded and have a discrete energy law. Proper numerical treatment of these properties is made difficult by the fact that the non-linearity occurs in the highest order derivative. Numerical algorithms are mainly designed so as to keep lower bounds and to be mass-preserving. We refer the reader to [20, 6, 25, 3, 23]. As far as we are concerned, there is no numerical method coping with a discrete energy law.

1.3. Notation. We collect here as a reference some standard notation used throughout the paper. For $p \in [1, \infty]$, we denote by $L^p(\Omega)$ the usual Lebesgue space, i.e.,

$$L^p(\Omega) = \{v : \Omega \rightarrow \mathbb{R} : v \text{ Lebesgue-measurable, } \int_{\Omega} |v(\mathbf{x})|^p d\mathbf{x} < \infty\}.$$

or

$$L^{\infty}(\Omega) = \{v : \Omega \rightarrow \mathbb{R} : v \text{ Lebesgue-measurable, } \text{ess sup}_{\mathbf{x} \in \Omega} |v(\mathbf{x})| < \infty\}.$$

This space is a Banach space endowed with the norm $\|v\|_{L^p(\Omega)} = (\int_{\Omega} |v(\mathbf{x})|^p d\mathbf{x})^{1/p}$ if $p \in [1, \infty)$ or $\|v\|_{L^{\infty}(\Omega)} = \text{ess sup}_{\mathbf{x} \in \Omega} |v(\mathbf{x})|$ if $p = \infty$. In particular, $L^2(\Omega)$ is a Hilbert space. We shall use $(u, v) = \int_{\Omega} u(\mathbf{x})v(\mathbf{x}) d\mathbf{x}$ for its inner product and $\|\cdot\|$ for its norm.

Let $\alpha = (\alpha_1, \alpha_2) \in \mathbb{N}^2$ be a multi-index with $|\alpha| = \alpha_1 + \alpha_2$, and let ∂^{α} be the differential operator such that

$$\partial^{\alpha} = \left(\frac{\partial}{\partial x_1} \right)^{\alpha_1} \left(\frac{\partial}{\partial x_2} \right)^{\alpha_2}.$$

For $m \geq 0$ and $p \in [1, \infty)$, we consider $W^{m,p}(\Omega)$ to be the Sobolev space of all functions whose m derivatives are in $L^p(\Omega)$, i.e.,

$$W^{m,p}(\Omega) = \{v \in L^p(\Omega) : \partial^k v \in L^2(\Omega) \forall |k| \leq m\}$$

associated to the norm

$$\|f\|_{W^{m,p}(\Omega)} = \left(\sum_{|\alpha| \leq m} \|\partial^{\alpha} f\|_{L^p(\Omega)}^p \right)^{1/p} \quad \text{for } 1 \leq p < \infty,$$

and

$$\|f\|_{W^{m,p}(\Omega)} = \max_{|\alpha| \leq m} \|\partial^{\alpha} f\|_{L^{\infty}(\Omega)} \quad \text{for } p = \infty.$$

For $p = 2$, we denote $W^{m,2}(\Omega) = H^m(\Omega)$. Moreover, we make of use the space

$$H_N^2(\Omega) = \{v \in H^2(\Omega) : \int_{\Omega} v(\mathbf{x}) d\mathbf{x} = 0 \text{ and } \partial_{\mathbf{n}} v = 0 \text{ on } \partial\Omega\},$$

for which is known that $\|v\|_{H_N^2(\Omega)}$ and $\|\Delta v\|$ are equivalent norms.

1.4. Outline. The remainder of this paper is organized in the following way. In the next section we state our finite element space and some tools. In particular, we prove a discrete version of a variant of Moser–Trudinger’s inequality. In section 4, we apply our ideas to discretize system (1) in space and time for defining our numerical method and formulate our main result. Next is section 5 dedicated to demonstrating lower bounds, a discrete energy law, and *a priori* bounds all of which are local in time for approximate solutions. This is accomplished in a series of lemmas where the final argument is an induction procedure on the time step so as to obtain the above mentioned properties globally in time. Finally, in section 6, we consider two numerical examples regarding blow-up and non blow-up scenarios.

2. TECHNICAL PRELIMINARIES

This section is mainly devoted to setting out the hypotheses and some auxiliary results concerning the finite element space that will use throughout this work.

2.1. Hypotheses. We construct the finite element approximation of (1) under the following assumptions on the domain, the mesh, and the finite element space.

- (H1) Let Ω be a convex, bounded domain of \mathbb{R}^2 with a polygonal boundary, and let θ_Ω be the minimum interior angle at the vertices of $\partial\Omega$.
- (H2) Let $\{\mathcal{T}_h\}_{h>0}$ be a family of acute, shape-regular, quasi-uniform triangulations of $\bar{\Omega}$ made up of triangles, so that $\bar{\Omega} = \cup_{T \in \mathcal{T}_h} T$, where $h = \max_{T \in \mathcal{T}_h} h_T$, with h_T being the diameter of T . More precisely, we assume that
 - (a) there exists $\alpha > 0$, independent of h , such that

$$\min\{\text{diam } B_T : T \in \mathcal{T}_h\} \geq \alpha h,$$

where B_T is the largest ball contained in T , and

- (b) there exists $\beta > 0$ such that every angle between two edges of a triangle T is bounded by $\frac{\pi}{2} - \beta$.

Further, let $\mathcal{N}_h = \{\mathbf{a}_i\}_{i \in I}$ be the coordinates of the nodes of \mathcal{T}_h .

- (H3) Associated with \mathcal{T}_h is the finite element space

$$X_h = \{x_h \in C^0(\bar{\Omega}) : x_h|_T \in \mathcal{P}_1(T), \forall T \in \mathcal{T}_h\},$$

where $\mathcal{P}_1(T)$ is the set of linear polynomials on T . Let $\{\varphi_{\mathbf{a}}\}_{\mathbf{a} \in \mathcal{N}_h}$ be the standard basis functions for X_h .

2.2. Auxiliary results. Our first result is concerned with the sign of the entries of the rigid matrix.

Proposition 2.1. *Let Ω be a polygonal. Consider X_h to be constructed over \mathcal{T}_h being acute. Then, for each $T \in \mathcal{T}_h$ with vertices $\{\mathbf{a}_1, \mathbf{a}_2, \mathbf{a}_3\}$, there exists a constant $C_{\text{neg}} > 0$, depending on β , but otherwise independent of h and T , such that*

$$(4) \quad \int_T \nabla \varphi_{\mathbf{a}_i} \cdot \nabla \varphi_{\mathbf{a}_j} d\mathbf{x} \leq -C_{\text{neg}}$$

for all $\mathbf{a}_i, \mathbf{a}_j \in T$ with $i \neq j$, and

$$(5) \quad \int_T \nabla \varphi_{\mathbf{a}_i} \cdot \nabla \varphi_{\mathbf{a}_i} d\mathbf{x} \geq C_{\text{neg}}$$

for all $\mathbf{a}_i \in T$.

A proof of (4) and (5) can be found in [10].

Both local and global finite element properties for X_h will be needed such as inverse estimates and bounds for the interpolation error. We first recall some local inverse estimates. See [2, Lem. 4.5.3] or [7, Lem. 1.138] for a proof.

Proposition 2.2. *Let Ω be polygonal. Consider X_h to be constructed over \mathcal{T}_h being quasi-uniform. Then, for each $T \in \mathcal{T}_h$ and $p \in [2, \infty]$, there exists a constant $C_{\text{inv}} > 0$, independent of h and T , such that, for all $x_h \in X_h$,*

$$(6) \quad \|\nabla x_h\|_{L^p(T)} \leq C_{\text{inv}} h^{-1} \|x_h\|_{L^p(T)}$$

and

$$(7) \quad \|\nabla x_h\|_{L^\infty(T)} \leq C_{\text{inv}} h^{-\frac{2}{p}} \|\nabla x_h\|_{L^p(T)}.$$

Concerning global inverse inequalities, we need the following.

Proposition 2.3. *Let Ω be polygonal. Consider X_h to be constructed over \mathcal{T}_h being quasi-uniform. Then for each $p \in [2, \infty]$, there exists a constant $C_{\text{inv}} > 0$, independent of h , such that, for all $x_h \in X_h$,*

$$(8) \quad \|x_h\|_{L^\infty(\Omega)} \leq C_{\text{inv}} h^{-1} \|x_h\|,$$

$$(9) \quad \|\nabla x_h\|_{L^p(\Omega)} \leq C_{\text{inv}} h^{-1} \|x_h\|_{L^p(\Omega)},$$

$$(10) \quad \|\nabla x_h\|_{L^p(\Omega)} \leq C_{\text{inv}} h^{-2(\frac{1}{2} - \frac{1}{p})} \|\nabla x_h\|_{L^2(\Omega)},$$

and

$$(11) \quad \|\nabla x_h\|_{L^\infty(\Omega)} \leq C_{\text{inv}} h^{-\frac{2}{p}} \|\nabla x_h\|_{L^p(\Omega)}.$$

We introduce $\mathcal{I}_h : C(\Omega) \rightarrow X_h$, the standard nodal interpolation operator, such that $\mathcal{I}_h \eta(\mathbf{a}) = \eta(\mathbf{a})$ for all $\mathbf{a} \in \mathcal{N}_h$. Associated with \mathcal{I}_h , a discrete inner product on X_h is defined by

$$(x_h, \bar{x}_h)_h = \int_{\Omega} \mathcal{I}_h(x_h(\mathbf{x})) \bar{x}_h(\mathbf{x}) \, d\mathbf{x}.$$

We also introduce

$$\|x_h\|_h = (x_h, x_h)^{\frac{1}{2}}.$$

Local and global error bounds for \mathcal{I}_h are as follows (c.f. [2, Thm. 4.4.4] or [7, Thm. 1.103] for a proof).

Proposition 2.4. *Let Ω be polygonal. Consider X_h to be constructed over \mathcal{T}_h being quasi-uniform. Then, for each $T \in \mathcal{T}_h$, there exists $C_{\text{app}} > 0$, independent of h and T , such that*

$$(12) \quad \|\varphi - \mathcal{I}_h \varphi\|_{L^1(T)} \leq C_{\text{app}} h^2 \|\nabla^2 \varphi\|_{L^1(T)} \quad \forall \varphi \in W^{2,1}(T).$$

Proposition 2.5. *Let Ω be polygonal. Consider X_h to be constructed over \mathcal{T}_h being quasi-uniform. Then it follows that there exists $C_{\text{app}} > 0$, independent of h , such that*

$$(13) \quad \|\nabla(\varphi - \mathcal{I}_h \varphi)\|_{L^2(\Omega)} \leq C_{\text{app}} h \|\Delta \varphi\|_{L^2(\Omega)} \quad \forall \varphi \in H^2(\Omega).$$

Corollary 2.6. *Let Ω be polygonal. Consider X_h to be constructed over \mathcal{T}_h being quasi-uniform. Let $n \in \mathbb{N}$. Then it follows that there exist three positive constants C_{app} , C_{com} , and C_{sta} , independent of h , such that*

$$(14) \quad \|x_h^n - \mathcal{I}_h(x_h^n)\|_{L^1(\Omega)} \leq C_{\text{app}} n(n-1) h^2 \int_{\Omega} |x_h(\mathbf{x})|^{n-2} |\nabla x_h(\mathbf{x})|^2 \, d\mathbf{x},$$

$$(15) \quad \|x_h \bar{x}_h - \mathcal{I}_h(x_h \bar{x}_h)\|_{L^1(\Omega)} \leq C_{\text{com}} h \|x_h\|_{L^2(\Omega)} \|\nabla \bar{x}_h\|_{L^2(\Omega)}$$

and

$$(16) \quad \|x_h^n\|_{L^1(\Omega)} \leq \|\mathcal{I}_h(x_h^n)\|_{L^1(\Omega)} \leq C_{\text{sta}} \|x_h^n\|_{L^1(\Omega)},$$

where C_{sta} depends on n .

Proof. Let $T \in \mathcal{T}_h$ and compute

$$\nabla^2(x_h^n) = n(n-1)x_h^{n-2} \sum_{i,j=1}^d \partial_i x_h \partial_j x_h \quad \text{on } T.$$

Then, from (12) and the above identity, we have

$$\begin{aligned} \|x_h^n - \mathcal{I}_h(x_h^k)\|_{L^1(T)} &\leq C_{\text{app}} h_K^2 \|\nabla^2(x_h^n)\|_{L^1(T)} \\ &\leq C_{\text{app}} n(n-1)h^2 \int_T |x_h(\mathbf{x})|^{n-2} |\nabla x_h(\mathbf{x})|^2 d\mathbf{x}. \end{aligned}$$

Summing over $T \in \mathcal{T}_h$ yields (14). The proof of (15) follows very closely the arguments of (14) for $n = 2$. The first part of assertion (16) is a simple application of Jensen's inequality, whereas the second part follows from (14) on using Hölder's inequality, (9) for $p = n$ and, later on, reverse Minkowski's inequality. \square

The proof of the following proposition can be found in [5]. It is a generalization of a Moser-Trudinger-type inequality.

Proposition 2.7 (Moser-Trudinger). *Let Ω be polygonal with θ_Ω being the minimum interior angle at the vertices of Ω . Then there exists a constant $C_\Omega > 0$ depending on Ω such that for all $u \in H^1(\Omega)$ with $\|\nabla u\| \leq 1$ and $\int_\Omega u(\mathbf{x}) d\mathbf{x} = 1$, it follows that*

$$(17) \quad \int_\Omega e^{\alpha|u(\mathbf{x})|^2} d\mathbf{x} \leq C_\Omega,$$

where $\alpha \leq 2\theta_\Omega$.

Corollary 2.8. *Let Ω be polygonal with θ_Ω being the minimum interior angle at the vertices of $\partial\Omega$. Consider X_h to be constructed over \mathcal{T}_h being quasi-uniform. Let $u_h \in X_h$ with $u_h > 0$. Then it follows that there exists a constant $C_{\text{MT}} > 0$, independent of h , such that*

$$(18) \quad \int_\Omega \mathcal{I}_h(e^{u_h(\mathbf{x})}) d\mathbf{x} \leq C_\Omega (1 + C_{\text{MT}} \|\nabla u_h\|^2) e^{\frac{1}{8\theta_\Omega} \|\nabla u_h\|^2} + \frac{1}{|\Omega|} \|u_h\|_{L^1(\Omega)}.$$

Proof. From (14), we have

$$\begin{aligned} (19) \quad \int_\Omega \mathcal{I}_h(e^{u_h(\mathbf{x})}) d\mathbf{x} &= \int_\Omega (1 + u_h(\mathbf{x})) d\mathbf{x} + \sum_{n=2}^{\infty} \frac{1}{n!} \int_\Omega \mathcal{I}_h(u_h^n(\mathbf{x})) d\mathbf{x} \\ &\leq \sum_{n=0}^{\infty} \frac{1}{n!} \int_\Omega u_h^n(\mathbf{x}) d\mathbf{x} \\ &\quad + \sum_{n=2}^{\infty} \frac{C_{\text{app}} n(n-1)h^2}{n!} \int_\Omega |\nabla u_h(\mathbf{x})|^2 u_h^{n-2}(\mathbf{x}) d\mathbf{x} \\ &= \int_\Omega (1 + C_{\text{app}} h^2 |\nabla u_h(\mathbf{x})|^2) e^{u_h(\mathbf{x})} d\mathbf{x}. \end{aligned}$$

Let $v_h = \frac{u_h - m}{\|\nabla u_h\|}$ with $m = \frac{1}{|\Omega|} \int_\Omega u_h(\mathbf{x}) d\mathbf{x}$. Young's inequality gives

$$(20) \quad u_h = \|\nabla u_h\| v_h + m \leq \frac{1}{8\theta_\Omega} \|\nabla u_h\|^2 + 2\theta_\Omega |v_h|^2 + m.$$

Thus, combining (19) and (20) yields, on noting (11) for $p = 2$ and (17), that

$$\begin{aligned} \int_\Omega \mathcal{I}_h(e^{u_h(\mathbf{x})}) d\mathbf{x} &\leq e^{\frac{1}{8\theta_\Omega} \|\nabla u_h\|^2 + m} \int_\Omega (1 + C_{\text{app}} h^2 \|\nabla u_h(\mathbf{x})\|^2 |\nabla v_h(\mathbf{x})|^2) e^{2\theta_\Omega |v_h(\mathbf{x})|^2} d\mathbf{x} \\ &\leq e^{\frac{1}{8\theta_\Omega} \|\nabla u_h\|^2 + m} (1 + C_{\text{app}} C_{\text{inv}} \|\nabla u_h(\mathbf{x})\|^2) \int_\Omega e^{2\theta_\Omega |v_h(\mathbf{x})|^2} d\mathbf{x} \\ &\leq C_\Omega (1 + C_{\text{app}} C_{\text{inv}} \|\nabla u_h(\mathbf{x})\|^2) e^{\frac{1}{8\theta_\Omega} \|\nabla u_h\|^2 + m}. \end{aligned}$$

□

An (average) interpolation operator into X_h will be required in order to properly initialize our numerical method. We refer to [21, 8].

Proposition 2.9. *Let Ω be polygonal. Consider X_h to be constructed over \mathcal{T}_h being quasi-uniform. Then there exists an (average) interpolation operator \mathcal{Q}_h from $L^1(\Omega)$ to X_h such that*

$$(21) \quad \|\mathcal{Q}_h \psi\|_{W^{s,p}(\Omega)} \leq C_{\text{sta}} \|\psi\|_{W^{s,p}(\Omega)} \quad \text{for } s = 0, 1 \text{ and } 1 \leq p \leq \infty,$$

and

$$(22) \quad \|\mathcal{Q}_h(\psi) - \psi\|_{W^{s,p}(\Omega)} \leq C_{\text{app}} h^{1+m-s} \|\psi\|_{W^{m+1,p}(\Omega)} \quad \text{for } 0 \leq s \leq m \leq 1.$$

Moreover, let $-\tilde{\Delta}_h$ be defined from X_h to X_h as

$$(23) \quad -(\tilde{\Delta}_h x_h, \bar{x}_h)_h = (\nabla x_h, \nabla \bar{x}_h) \quad \text{for all } \bar{x}_h \in X_h,$$

and let $x(h) \in H_N^2(\Omega)$ be such that

$$(24) \quad \begin{cases} -\Delta x(h) &= -\tilde{\Delta}_h x_h & \text{in } \Omega, \\ \partial_n x(h) &= 0 & \text{on } \partial\Omega. \end{cases}$$

From elliptic regularity theory, the well-posedness of (24) is ensured by the convexity assumption stated in (H1) and

$$(25) \quad \|x(h)\|_{H_N^2(\Omega)} \leq C \| -\tilde{\Delta}_h x_h \|.$$

See [9] for a proof.

Proposition 2.10. *Let Ω be a convex polygon. Consider X_h to be constructed over \mathcal{T}_h being quasi-uniform. Then there exists a constant $C_{\text{Lap}} > 0$, independent of h , such that*

$$(26) \quad \|\nabla(x(h) - x_h)\|_{L^2(\Omega)} \leq C_{\text{Lap}} h \|\tilde{\Delta}_h x_h\|_{L^2(\Omega)}.$$

Proof. We refer the reader to [10] for a proof which uses (13) and (15). □

Corollary 2.11. *Let Ω be a convex polygon. Consider X_h to be constructed over \mathcal{T}_h being quasi-uniform. Then, for each $p \in [2, \infty]$, there exists a constant $C_{\text{sta}} > 0$, independent of h , such that*

$$(27) \quad \|\nabla x_h\|_{L^p(\Omega)} \leq C_{\text{sta}} \| -\tilde{\Delta}_h x_h \|.$$

Proof. The triangle inequality gives

$$\|\nabla x_h\|_{L^p(\Omega)} \leq \|\nabla x_h - \nabla \mathcal{Q}_h x(h)\|_{L^p(\Omega)} + \|\nabla \mathcal{Q}_h x(h)\|_{L^p(\Omega)}$$

and hence applying (10), (26), (25), (22), (21), and Sobolev's inequality yields (27). □

3. PRESENTATION OF MAIN RESULT

We now define our numerical approximation of system (1). Assume that $(u_0, v_0) \in H^1(\Omega) \times H^2(\Omega)$ with $u_0 > 0$ and $v_0 \geq 0$ a. e. in Ω .

We begin by approximating the initial data (u_0, v_0) by $(u_h^0, v_h^0) \in X_h^2$ as follows. Define

$$(28) \quad u_h^0 = \mathcal{Q}_h u_0,$$

which satisfies

$$(29) \quad u_h^0 > 0 \text{ a. e. in } \Omega, \quad \|u_h^0\|_{L^1(\Omega)} \leq C_{\text{sta}} \|u_0\|_{L^1(\Omega)} \quad \text{and} \quad \|u_h^0\| \leq C_{\text{sta}} \|u_0\|$$

and

$$(30) \quad v_h^0 = \mathcal{Q}_h v_0,$$

which satisfies

$$(31) \quad v_h^0 \geq 0 \text{ a. e. in } \Omega, \quad \|v_h^0\|_{H^1(\Omega)} \leq C \|v_0\|_{H^1(\Omega)} \quad \text{and} \quad \|\tilde{\Delta}_h v_h^0\| \leq C \|\Delta v_0\|.$$

Given $N \in \mathbb{N}$, we let $0 = t_0 < t_1 < \dots < t_{N-1} < t_N = T$ be a uniform partitioning of $[0, T]$ with time step $k = \frac{T}{N}$. To simplify the notation we define the time-increment operator $\delta_t \phi_h^{n+1} = \frac{\phi_h^{n+1} - \phi_h^n}{k}$.

Known $(u_h^n, v_h^n) \in X_h \times X_h$, find $(u_h^{n+1}, v_h^{n+1}) \in X_h \times X_h$ such that

$$(32) \quad (\delta_t u_h^{n+1}, x_h)_h + (\nabla u_h^{n+1}, \nabla x_h) = (\nabla v_h^n, u_h^{n+1} \nabla x_h)$$

and

$$(33) \quad (\delta_t v_h^{n+1}, x_h)_h + (\nabla v_h^{n+1}, \nabla x_h) + (v_h^{n+1}, x_h)_h = (u_h^{n+1}, x_h)_h.$$

It should be noted that scheme (32)-(33) combines a finite element method together a mass-lumping technique to treat some terms and a semi-implicit time integrator. The resulting scheme is linear and decouples the computation of u_h^{n+1} and v_h^{n+1} .

In order to carry out our numerical analysis we must rewrite the chemotaxis term by using a barycentric quadrature rule as follows. Let $T \in \mathcal{T}_h$ and consider $\mathbf{b}_T \in T$ to be the barycentre of T . Then let \bar{u}_h^{n+1} be the interpolation of u_h^{n+1} into X_h^0 , with X_h^0 being the space of all piecewise constant functions over \mathcal{T}_h , defined by

$$(34) \quad \bar{u}_h^{n+1}|_T = u_h^{n+1}(\mathbf{b}_T).$$

As a result, one has

$$(35) \quad (\nabla v_h^n, u_h^{n+1} \nabla x_h) = \sum_{T \in K} |T| \nabla v_h^n \cdot \nabla x_h u_h^{n+1}(\mathbf{b}_T) = (\nabla v_h^n, \bar{u}_h^{n+1} \nabla x_h).$$

From now on we will use C to denote a generic constant independent of the discretization parameters (h, k) .

Let us define

$$(36) \quad \mathcal{E}_0(u_h, v_h) = \frac{1}{2} \|v_h\|_h^2 + \frac{1}{2} \|\nabla v_h\|^2 - (u_h, v_h)_h + (\log u_h, u_h)_h,$$

$$(37) \quad \mathcal{E}_1(u_h, v_h) = \|u_h\|_h^2 + \|\tilde{\Delta}_h v_h\|^2.$$

and, for each $\varepsilon, \delta \in (0, 1)$,

$$(38) \quad \mathcal{R}_0^{\varepsilon, \delta}(u_h^0, v_h^0) := \frac{1}{\delta e} + \frac{\|u_h^0\|_{L^1(\Omega)}}{\delta} \left(\frac{C_\Omega}{\varepsilon} + \varepsilon + \frac{(1+\delta)}{|\Omega|} (\|v_h^0\|_{L^1(\Omega)} + \|u_h^0\|_{L^1(\Omega)}) \right).$$

Associated with the above definitions, consider

$$\begin{aligned} \mathcal{B}_0(u_h, v_h) &= \frac{1}{\delta} \mathcal{E}_0(u_h, v_h) + \mathcal{R}_0^{\delta, \varepsilon}(u_h, v_h), \\ \mathcal{B}_1(u_h, v_h) &= (1 + \frac{1}{\delta}) \mathcal{E}_0(u_h, v_h) + \mathcal{R}_0^{\delta, \varepsilon}(u_h, v_h) + 2 \frac{|\Omega|}{e}, \end{aligned}$$

and

$$\mathcal{B}_2(u_h, v_h) = \mathcal{E}_0(u_h, v_h) + \mathcal{B}_0(u_h, v_h) + \mathcal{B}_1(u_h, v_h).$$

Finally, define

$$\mathcal{F}(u_h, v_h) = e^{\mathcal{B}_2(u_h, v_h) + T^{\frac{1}{2}} \mathcal{B}_2^{\frac{1}{2}}(u_h, v_h)} (\mathcal{E}_0(u_h, v_h) + CT \mathcal{B}_1^3(u_h, v_h) + CT \|u_h\|_{L^1(\Omega)}).$$

The definition of the above quantities will be apparent later.

We are now prepared to state the main result of this paper.

Theorem 3.1. *Assume that hypotheses (H1)–(H3) are satisfied. Let $(u_0, v_0) \in H^1(\Omega) \times H_N^2(\Omega)$ with $u_0 > 0$ and $v_0 \geq 0$, and take $u_h^0 > 0$ and $v_h^0 \geq 0$ defined by (28) and (30), respectively. Assume that (h, k) fulfill*

$$(39) \quad C \frac{k}{h^2} \mathcal{F}(u_h^0, v_h^0) < \frac{1}{2}$$

and

$$(40) \quad -C_{\text{neg}} + Ch^{1-\frac{2}{p}} \mathcal{F}^{\frac{1}{2}}(u_h^0, v_h^0) < 0.$$

Then the sequence $\{(u_h^m, v_h^m)\}_{m=0}^N$ computed via (32) and (33) satisfies the following properties, for all $m \in \{0, \dots, N\}$:

- Lower bounds:

$$(41) \quad u_h^m(\mathbf{x}) > 0$$

and

$$(42) \quad v_h^m(\mathbf{x}) \geq 0$$

for all $\mathbf{x} \in \Omega$,

- $L^1(\Omega)$ -bounds:

$$(43) \quad \|u_h^m\|_{L^1(\Omega)} = \|u_h^0\|_{L^1(\Omega)}$$

and

$$(44) \quad \|v_h^m\|_{L^1(\Omega)} \leq \|v_h^0\|_{L^1(\Omega)} + \|u_h^0\|_{L^1(\Omega)}.$$

- A discrete energy law:

$$(45) \quad \mathcal{E}_0(u_h^m, v_h^m) + k \sum_{r=1}^m (\|\delta_t v_h^r\|_h^2 + k \|\mathcal{A}_h^{-\frac{1}{2}}(u_h^r) \nabla u_h^r - \mathcal{A}_h^{\frac{1}{2}}(u_h^r) \nabla v_h^{r-1}\|^2) \leq \mathcal{E}_0(u_h^0, v_h^0),$$

where \mathcal{A}_h is defined in (61).

Moreover, if we are given h such that

$$(46) \quad Ch^{1-\frac{2}{p}} \mathcal{E}_1(u_h^0, v_h^0) \leq \frac{5}{12},$$

it follows that

$$(47) \quad \mathcal{E}_1(u_h^m, v_h^m) + \frac{k}{2} \sum_{r=1}^m (\|\nabla u_h^r\|^2 + \|\nabla \tilde{\Delta}_h v_h^r\|^2) \leq \mathcal{F}(u_h^0, v_h^0).$$

As system (32)-(33) is linear, existence follows from uniqueness. The latter is an immediate outcome of *a priori* bounds for (u_h^{n+1}, v_h^{n+1}) .

4. PROOF OF MAIN RESULT

In this section we address the proof of Theorem 3.1. Rather than prove *en masse* the estimates in Theorem 3.1, because all of them are connected, we have divided the proof into various subsections for the sake of clarity. The final argument will be an induction procedure on n relied on the semi-explicit time discretization employed in (32).

4.1. Lower bounds and a discrete energy law. We first demonstrate lower bounds for (u_h^{n+1}, v_h^{n+1}) and, as a consequence of this, a discrete local-in-time energy law is established.

Lemma 4.1 (Lower bounds). *Assume that (H1)–(H3) are satisfied. Let $u_h^n > 0$ and $v_h^n \geq 0$ and let*

$$(48) \quad \|\tilde{\Delta}_h v_h^n\|^2 \leq \mathcal{F}(u_h^0, v_h^0).$$

Then if one chooses (h, k) satisfying (39) and (40), it follows that the solution $(u_h^{n+1}, v_h^{n+1}) \in X_h^2$ computed via (32) and (33) are lower bounded, i.e., for all $\mathbf{x} \in \Omega$,

$$(49) \quad u_h^{n+1}(\mathbf{x}) > 0$$

and

$$(50) \quad v_h^{n+1}(\mathbf{x}) \geq 0.$$

Proof. Since u_h^{n+1} and v_h^{n+1} are piecewise linear polynomial functions, it will suffice to prove that (49) and (50) hold at the nodes. To do this, let $T \in \mathcal{T}_h$ be a fixed triangle with vertices $\{\mathbf{a}_1, \mathbf{a}_2, \mathbf{a}_3\}$, and choose two of them, i.e. $\mathbf{a}_i, \mathbf{a}_j \in T$ with $i \neq j$. Then, from (6) for $p = \infty$, (7), (27), and (48), we have on noting (35) that

$$\begin{aligned} \int_T \bar{\varphi}_{\mathbf{a}_i} \nabla v_h^n \cdot \nabla \varphi_{\mathbf{a}_j} \, d\mathbf{x} &= \int_T \varphi_{\mathbf{a}_i}(\mathbf{b}_T) \nabla v_h^n \cdot \nabla \varphi_{\mathbf{a}_j} \, d\mathbf{x} \\ (51) \quad &\leq |T| \|\varphi_{\mathbf{a}_i}\|_{L^\infty(T)} \|\nabla v_h^n\|_{L^\infty(T)} \|\nabla \varphi_{\mathbf{a}_j}\|_{L^\infty(T)} \\ &\leq Ch \|\nabla v_h^n\|_{L^\infty(T)} \leq Ch^{1-\frac{2}{p}} \|\nabla v_h^n\|_{L^p(T)} \\ &\leq Ch^{1-\frac{2}{p}} \|\tilde{\Delta}_h v_h^n\|_{L^2(\Omega)} \leq Ch^{1-\frac{2}{p}} \mathcal{F}_0^{\frac{1}{2}}(u_h^0, v_h^0). \end{aligned}$$

If we now compare (4) with (51), we find on recalling (40) that

$$\begin{aligned} \int_T \nabla \varphi_{\mathbf{a}_i} \cdot \nabla \varphi_{\mathbf{a}_j} \, d\mathbf{x} - \int_T \bar{\varphi}_{\mathbf{a}_i} \nabla v_h^n \cdot \nabla \varphi_{\mathbf{a}_j} \, d\mathbf{x} \\ \leq -C_{\text{neg}} + Ch^{1-\frac{2}{p}} \mathcal{F}_0^{\frac{1}{2}}(u_h^0, v_h^0) < 0 \end{aligned}$$

and on summing over $T \in \text{supp } \varphi_{\mathbf{a}_i} \cap \text{supp } \varphi_{\mathbf{a}_j}$ that

$$(52) \quad (\nabla \varphi_{\mathbf{a}_i}, \nabla \varphi_{\mathbf{a}_j}) - (\bar{\varphi}_{\mathbf{a}_i} \nabla v_h^n, \nabla \varphi_{\mathbf{a}_j}) < 0.$$

Analogously, we have, from (5), that

$$(53) \quad (\nabla \varphi_{\mathbf{a}_i}, \nabla \varphi_{\mathbf{a}_i}) - (\bar{\varphi}_{\mathbf{a}_i} \nabla v_h^n, \nabla \varphi_{\mathbf{a}_i}) > 0$$

holds under assumption (40).

Let $u_h^{\min} \in X_h$ be defined as

$$u_h^{\min} = \sum_{\mathbf{a} \in \mathcal{N}_h} u_h^-(\mathbf{a}) \varphi_{\mathbf{a}},$$

where $u_h^-(\mathbf{a}) = \min\{0, u_h^{n+1}(\mathbf{a})\}$. Analogously, one defines $u_h^{\max} \in X_h$ as

$$u_h^{\max} = \sum_{\mathbf{a} \in \mathcal{N}_h} u_h^+(\mathbf{a}) \varphi_{\mathbf{a}},$$

where $u_h^+(\mathbf{a}) = \max\{0, u_h^{n+1}(\mathbf{a})\}$. It is easy to check that $u_h^{n+1} = u_h^{\min} + u_h^{\max}$.

Set $\bar{x}_h = u_h^{\min}$ in (32) using (35) to get

$$(54) \quad (\delta_t u_h^{n+1}, u_h^{\min})_h + (\nabla u_h^{n+1}, \nabla u_h^{\min}) - (\bar{u}_h^{n+1} \nabla v_h^n, \nabla u_h^{\min}) = 0.$$

Our goal is to show that $u_h^{\min} \equiv 0$. Indeed, note that

$$(u_h^{n+1}, u_h^{\min})_h = (u_h^{\min} + u_h^{\max}, u_h^{\min})_h = \|u_h^{\min}\|_h^2.$$

and hence

$$(55) \quad (\delta_t u_h^{n+1}, u_h^{\min})_h = \frac{1}{k} \|u_h^{\min}\|_h^2 - \frac{1}{k} (u_h^n, u_h^{\min}) \geq \|u_h^{\min}\|_h^2,$$

where we have used the fact that $u_h^n > 0$. One can further write

$$\begin{aligned} &(\nabla u_h^{n+1}, \nabla u_h^{\min}) - (\bar{u}_h^{n+1} \nabla v_h^n, \nabla u_h^{\min}) \\ &= (\nabla u_h^{\max}, \nabla u_h^{\min}) - (\bar{u}_h^{\max} \nabla v_h^n, \nabla u_h^{\min}) \\ &\quad + (\nabla u_h^{\min}, \nabla u_h^{\min}) - (\bar{u}_h^{\min} \nabla v_h^n, \nabla u_h^{\min}), \end{aligned}$$

whereupon we deduce from (52) and (53) that

$$\begin{aligned} &(\nabla u_h^{\max}, \nabla u_h^{\min}) - (\bar{u}_h^{\max} \nabla v_h^n, \nabla u_h^{\min}) \\ &= \sum_{\mathbf{a} \neq \tilde{\mathbf{a}} \in \mathcal{N}_h} u_h^{\max}(\mathbf{a}) u_h^{\min}(\tilde{\mathbf{a}}) \left[(\nabla \varphi_{\mathbf{a}}, \nabla \varphi_{\tilde{\mathbf{a}}}) - (\bar{\varphi}_{\mathbf{a}} \nabla v_h^n, \nabla \varphi_{\tilde{\mathbf{a}}}) \right] \\ &\quad + \sum_{\mathbf{a} \in \mathcal{N}_h} u_h^{\max}(\mathbf{a}) u_h^{\min}(\mathbf{a}) \left[(\nabla \varphi_{\mathbf{a}}, \nabla \varphi_{\mathbf{a}}) - (\bar{\varphi}_{\mathbf{a}} \nabla v_h^n, \nabla \varphi_{\mathbf{a}}) \right] \geq 0, \end{aligned}$$

since $u_h^{\max}(\mathbf{a})u_h^{\min}(\tilde{\mathbf{a}}) \leq 0$ and $u_h^{\max}(\mathbf{a})u_h^{\min}(\mathbf{a}) = 0$. Therefore,

$$(56) \quad (\nabla u_h^{\min}, \nabla u_h^{\min}) - (\bar{u}_h^{\min} \nabla v_h^n, \nabla u_h^{\min}) \leq (\nabla u_h^{n+1}, \nabla u_h^{\min}) - (\bar{u}_h^{n+1} \nabla v_h^n, \nabla u_h^{\min})$$

As a result, we infer on applying (55) and (56) into (54) that

$$\|u_h^{\min}\|_h^2 + k\|\nabla u_h^{\min}\|^2 \leq k(\bar{u}_h^{\min} \nabla v_h^n, \nabla u_h^{\min}).$$

But inequalities (8), (16) for $n = 2$, (27) for $p = 2$, (48), and (39) allow us to estimate

$$\begin{aligned} \|u_h^{\min}\|_h^2 + k\|\nabla u_h^{\min}\|^2 &\leq k\|u_h^{\min}\|_{L^\infty(\Omega)}\|\nabla v_h^n\|_{L^2(\Omega)}\|\nabla u_h^{\min}\|^2 \\ &\leq C\frac{k}{h^2}\mathcal{F}(u_h^0, v_h^0)\|u_h^{\min}\|_h^2 + \frac{k}{2}\|\nabla u_h^{\min}\|^2 \\ &\leq \frac{1}{2}\|u_h^{\min}\|_h^2 + \frac{k}{2}\|\nabla u_h^{\min}\|^2; \end{aligned}$$

thereby

$$\|u_h^{\min}\|_h^2 \leq 0,$$

which, in turn, implies that $u_h^{\min} \equiv 0$ and hence $u_h^{n+1} \geq 0$. It remains to prove that indeed $u_h^{n+1} > 0$. We proceed by contradiction. Let $\tilde{\mathbf{a}} \in \mathcal{N}_h$ be such $u_h^{n+1}(\tilde{\mathbf{a}}) = 0$. Substitute $\bar{x}_h = \varphi_{\tilde{\mathbf{a}}}$ into (32) to arrive at

$$\begin{aligned} 0 < u_h^n(\tilde{\mathbf{a}}) \int_{\Omega} \varphi_{\tilde{\mathbf{a}}} &= (\nabla u_h^{n+1}, \nabla \varphi_{\tilde{\mathbf{a}}}) - (\nabla v_h^n, \bar{u}_h^{n+1} \nabla \varphi_{\tilde{\mathbf{a}}}) \\ &= \sum_{\tilde{\mathbf{a}} \neq \mathbf{a} \in \mathcal{N}_h} u_h^{n+1}(\mathbf{a}) \left\{ (\nabla \varphi_{\mathbf{a}}, \nabla \varphi_{\tilde{\mathbf{a}}}) - (\bar{\varphi}_{\mathbf{a}} \nabla v_h^n, \nabla \varphi_{\tilde{\mathbf{a}}}) \right\} \leq 0. \end{aligned}$$

In the last line we have utilized (52) and the fact that $u_h^{n+1} \geq 0$. This gives a contradiction.

It is now a simple matter to show that (50) holds. It completes the proof. \square

We are now concerned with obtaining $L^1(\Omega)$ bounds for (u_h^{n+1}, v_h^{n+1}) . In particular, we will see that equation (32) is mass-preserving.

Lemma 4.2 ($L^1(\Omega)$ -bounds). *Under the conditions of Lemma 4.1, the discrete solution pair $(u_h^{n+1}, v_h^{n+1}) \in X_h^2$ computed via (32) and (33) fulfills*

$$(57) \quad \|u_h^{n+1}\|_{L^1(\Omega)} = \|u_h^0\|_{L^1(\Omega)}$$

and

$$(58) \quad \|v_h^{n+1}\|_{L^1(\Omega)} \leq \|v_h^0\|_{L^1(\Omega)} + \|u_h^0\|_{L^1(\Omega)}.$$

Proof. On choosing $x_h = 1$ in (32), it follows immediately after a telescoping cancellation that

$$(59) \quad \int_{\Omega} u_h^{n+1}(\mathbf{x}) \, d\mathbf{x} = \int_{\Omega} u_h^0(\mathbf{x}) \, d\mathbf{x}.$$

Consequently, we get that (57) holds from (49) and (29). Now let $x_h = 1$ in (33) to get

$$\int_{\Omega} v_h^{n+1}(\mathbf{x}) \, d\mathbf{x} + k \int_{\Omega} v_h^{n+1}(\mathbf{x}) \, d\mathbf{x} = \int_{\Omega} v_h^n(\mathbf{x}) \, d\mathbf{x} + k \int_{\Omega} u_h^{n+1}(\mathbf{x}) \, d\mathbf{x}.$$

A simple calculation shows that

$$\int_{\Omega} v_h^{n+1}(\mathbf{x}) \, d\mathbf{x} = \frac{1}{(1+k)^{n+1}} \int_{\Omega} v_h^0(\mathbf{x}) \, d\mathbf{x} + \left(\int_{\Omega} u_h^0(\mathbf{x}) \, d\mathbf{x} \right) \sum_{j=1}^{n+1} \frac{k}{(1+k)^j},$$

where we have used (59). Inequality (58) is proved by applying (50). \square

Once the positivity of u_h^{n+1} has been proved, we are in a position to reformulate equation (32) so as to be able to obtain a discrete energy law, which exactly mimics its counterpart at the continuous level.

Lemma 4.3. *Under the conditions of Lemma 4.1. Equation (32) can be equivalently written as*

$$(60) \quad (\delta_t u_h^{n+1}, x_h)_h + (\nabla u_h^{n+1}, \nabla x_h) = (\nabla v_h^n, \mathcal{A}_h(u_h^{n+1}) \nabla x_h),$$

where $\mathcal{A}_h(u_h^{n+1}) \in \mathbb{R}^{2 \times 2}$ is a piecewise constant, diagonal matrix defined as follows. Let $T \in \mathcal{T}_h$. Then there exist two pairs $(\mathbf{a}_{\underline{u}^i}^T, \mathbf{a}_{\bar{u}^i}^T) \in T^2$, $i = 1, 2$, such that

$$(61) \quad [\mathcal{A}_h(u_h^{n+1})|_T]_{ii} = \begin{cases} \frac{u_h^{n+1}(\mathbf{a}_{\bar{u}^i}^T) - u_h^{n+1}(\mathbf{a}_{\underline{u}^i}^T)}{f'(u_h^{n+1}(\mathbf{a}_{\bar{u}^i}^T)) - f'(u_h^{n+1}(\mathbf{a}_{\underline{u}^i}^T))} & \text{if } u_h^{n+1}(\mathbf{a}_{\underline{u}^i}^T) - u_h^{n+1}(\mathbf{a}_{\bar{u}^i}^T) \neq 0, \\ u_h^{n+1}(\mathbf{b}_T) & \text{if } u_h^{n+1}(\mathbf{a}_{\underline{u}^i}^T) - u_h^{n+1}(\mathbf{a}_{\bar{u}^i}^T) = 0, \end{cases}$$

where $f(s) = s \log s - s$.

Proof. We must identify $\mathcal{A}_h(u_h^{n+1}) \equiv I_2 \bar{u}_h^{n+1}$, where I_2 is the 2×2 identity matrix. To do so, first observe that $f'(s) = \log s$. Then it is easy to see that, for each $\varepsilon > 0$ and $c \in (0, \infty)$, there exist two points $0 < \underline{u} < \bar{u}$ such that $|\underline{u} - \bar{u}| < \varepsilon$, with $\underline{u} \leq c \leq \bar{u}$, so that

$$\frac{f'(\bar{u}) - f'(\underline{u})}{\bar{u} - \underline{u}} = \frac{1}{c}.$$

Let $T \in \mathcal{T}_h$ and choose $c = u_h^{n+1}(\mathbf{b}_T)$. We are allowed to choose ε small enough such that

$$\underline{u} \geq \min_{t \in (-1, 1)} u_h^{n+1}(\mathbf{b}_T + r_{\mathbf{b}_T} \mathbf{e}_i t) \neq \max_{t \in (-1, 1)} u_h^{n+1}(\mathbf{b}_T + r_{\mathbf{b}_T} \mathbf{e}_i t) \geq \bar{u},$$

where $r_{\mathbf{b}_T} = \text{dist}(\mathbf{b}_T, \partial T)$ and \mathbf{e}_i is the i th vector of the canonical basis of \mathbb{R}^2 . Therefore, there exists a pair $(\mathbf{a}_{\underline{u}^i}^T, \mathbf{a}_{\bar{u}^i}^T)$ such that $u_h^{n+1}(\mathbf{a}_{\underline{u}^i}^T) = \underline{u}$ and $u_h^{n+1}(\mathbf{a}_{\bar{u}^i}^T) = \bar{u}$ and hence one defines

$$[\mathcal{A}_h(u_h^{n+1})|_T]_{ii} = \frac{u_h^{n+1}(\mathbf{a}_{\bar{u}^i}^T) - u_h^{n+1}(\mathbf{a}_{\underline{u}^i}^T)}{f'(u_h^{n+1}(\mathbf{a}_{\bar{u}^i}^T)) - f'(u_h^{n+1}(\mathbf{a}_{\underline{u}^i}^T))}.$$

In the case that $\min_{t \in (-1, 1)} u_h^{n+1}(\mathbf{b}_T + r_{\mathbf{b}_T} \mathbf{e}_i t) = \max_{t \in (-1, 1)} u_h^{n+1}(\mathbf{b}_T + r_{\mathbf{b}_T} \mathbf{e}_i t)$, one defines

$$[\mathcal{A}_h(u_h^{n+1})|_T]_{ii} = u_h^{n+1}(\mathbf{b}_T).$$

This completes the proof. \square

It is now shown that system (32)-(33) enjoys a discrete energy law locally in time.

Lemma 4.4 (A discrete energy law). *Under the conditions of Lemma 4.1, the discrete solution $(u_h^{n+1}, v_h^{n+1}) \in X_h^2$ computed via (32) and (33) satisfies*

$$(62) \quad \begin{aligned} & \mathcal{E}_0(u_h^{n+1}, v_h^{n+1}) - \mathcal{E}_0(u_h^n, v_h^n) + k \|\delta_t v_h^{n+1}\|_h^2 \\ & + k \|\mathcal{A}_h^{-\frac{1}{2}}(u_h^{n+1}) \nabla u_h^{n+1} - \mathcal{A}_h^{\frac{1}{2}}(u_h^{n+1}) \nabla v_h^n\|^2 \leq 0 \end{aligned}$$

where $\mathcal{E}_0(\cdot, \cdot)$ is defined in (36).

Proof. First of all, recall that $f(s) = s \log s - s$; therefore, we are allowed to compute $f'(u_h^{n+1})$ due to (49). Select $x_h = \mathcal{I}_h f'(u_h^{n+1}) - v_h^n$ in (60) and $x_h = \delta_t v_h^{n+1}$ in (33) to get

$$(63) \quad \begin{aligned} & (\delta_t u_h^{n+1}, f'(u_h^{n+1}) - v_h^n)_h + (\nabla u_h^{n+1}, \nabla (\mathcal{I}_h f'(u_h^{n+1}) - v_h^n)) \\ & - (\nabla v_h^n, \mathcal{A}_h(u_h^{n+1}) \nabla (\mathcal{I}_h f'(u_h^{n+1}) - v_h^n)) = 0 \end{aligned}$$

and

$$(64) \quad \begin{aligned} & \frac{1}{2k} (\|v_h^{n+1}\|_h^2 + \|\nabla v_h^{n+1}\|^2) - \frac{1}{2k} (\|v_h^n\|_h^2 + \|\nabla v_h^n\|^2) \\ & + \frac{1}{2k} \|v_h^{n+1} - v_h^n\|_h^2 + \frac{1}{2k} \|\nabla (v_h^{n+1} - v_h^n)\|^2 + \|\delta_t v_h^{n+1}\|_h^2 - (u_h^{n+1}, \delta_t v_h^{n+1})_h = 0. \end{aligned}$$

We next pair some terms from (63) and (64) in order to handle them together. It is not hard to see that

$$(65) \quad - (\delta_t u_h^{n+1}, v_h^n)_h - (u_h^{n+1}, \delta_t v_h^{n+1})_h = -\frac{1}{k} (u_h^{n+1}, v_h^{n+1})_h - \frac{1}{k} (u_h^n, v_h^n)_h.$$

In view of (61), there holds

$$\partial_{x_i} \mathcal{I}_h(f'(u_h^{n+1})) = \frac{f'(u_h^{n+1}(\mathbf{a}_{\bar{u}^i}^T)) - f'(u_h^{n+1}(\mathbf{a}_{\underline{u}^i}^T))}{[\mathbf{a}_{\bar{u}^i}^T - \mathbf{a}_{\underline{u}^i}^T]_i},$$

since \mathcal{I}_h is piecewise linear. As a result, one deduces from (61) that

$$\nabla \mathcal{I}_h f'(u_h^{n+1}) = \mathcal{A}_h^{-1}(u_h^{n+1}) \nabla u_h^{n+1}.$$

Therefore,

$$(\nabla u_h^{n+1}, \nabla (\mathcal{I}_h f'(u_h^{n+1}) - v_h^n)) = (\nabla u_h^{n+1}, \mathcal{A}_h^{-1}(u_h^{n+1}) \nabla u_h^{n+1}) - (\nabla u_h^{n+1}, \nabla v_h^n)$$

and

$$(\nabla v_h^n, \mathcal{A}_h(u_h^{n+1}) \nabla (\mathcal{I}_h f'(u_h^{n+1}) - v_h^n)) = (\nabla v_h^n, \nabla u_h^{n+1}) - (\nabla v_h^n, \mathcal{A}_h(u_h^{n+1}) \nabla v_h^n),$$

which imply that

$$(66) \quad \begin{aligned} & (\nabla u_h^{n+1}, \nabla (\mathcal{I}_h f'(u_h^{n+1}) - v_h^n)) - (\nabla v_h^n, \mathcal{A}_h(u_h^{n+1}) \nabla (\mathcal{I}_h f'(u_h^{n+1}) - v_h^n)) \\ &= \|\mathcal{A}_h^{-\frac{1}{2}}(u_h^{n+1}) \nabla u_h^{n+1} - \mathcal{A}_h^{-\frac{1}{2}}(u_h^{n+1}) \nabla v_h^n\|^2. \end{aligned}$$

A Taylor polynomial of f round u_h^{n+1} evaluated at u_h^n yields

$$f(u_h^n) = f(u_h^{n+1}) - f'(u_h^{n+1})(u_h^{n+1} - u_h^n) + \frac{f''(u_h^{n+\theta})}{2}(u_h^{n+1} - u_h^n)^2,$$

where $\theta \in (0, 1)$ such that $u_h^{n+\theta} = \theta u_h^{n+1} + (1 - \theta)u_h^n$. Hence,

$$(\partial_t u_h^{n+1}, f'(u_h^{n+1}))_h = \frac{1}{k}(f(u_h^{n+1}), 1)_h - \frac{1}{k}(f(u_h^{n+1}), 1)_h + \frac{k}{2}(f''(u_h^{n+\theta}), (\delta_t u_h^{n+1})^2)_h.$$

In fact, one can write the above expression as

$$(67) \quad (\partial_t u_h^{n+1}, f'(u_h^{n+1}))_h = (u_h^{n+1}, \log u_h^{n+1})_h - (u_h^n, \log u_h^n)_h + k(f''(u_h^{n+\theta}), (\delta_t u_h^{n+1})^2)_h$$

owing to

$$\int_{\Omega} u_h^{n+1}(\mathbf{x}) \, d\mathbf{x} = \int_{\Omega} u_h^n(\mathbf{x}) \, d\mathbf{x}.$$

On adding (63) and (64), we verify (62) from (65), (66), and (67). \square

4.2. *A priori* bounds. Now that we have accomplished the discrete energy law (62) for system (32)–(33), our goal is to derive *a priori* energy bounds. It will be no means obvious since $\mathcal{E}_0(u_h^{n+1}, v_h^{n+1})$ does not provide directly any control over u_h^{n+1} and v_h^{n+1} . The key ingredient will be the discrete Moser–Trudinger inequality (18).

Lemma 4.5 (Control of $(u_h^{n+1}, v_h^{n+1})_h$). *Assume that the conditions of Lemma 4.1 are satisfied. Let $u_0 \in H^1(\Omega)$ such that $\|u_0\|_{L^1(\Omega)} \in (0, 4\theta_{\Omega})$. Then there exist $\delta, \varepsilon \in (0, 1)$ such that*

$$(68) \quad (u_h^{n+1}, v_h^{n+1})_h \leq \frac{1}{\delta} \mathcal{E}_0(u_h^{n+1}, v_h^{n+1}) + \mathcal{R}_0^{\varepsilon, \delta}(u_h^0, v_h^0),$$

where $\mathcal{E}_0(\cdot, \cdot)$ and $\mathcal{R}_0^{\varepsilon, \delta}(\cdot, \cdot)$ are given in (36) and (38), respectively.

Proof. Let $\delta, \varepsilon \in (0, 1)$ such that

$$(69) \quad \frac{(1 + \delta)^2 [8\theta_{\Omega} C_{\text{MT}} \varepsilon + 1] \|u_0\|_{L^1(\Omega)}}{8\theta_{\Omega}} \leq \frac{1}{2}.$$

Using Jensen's inequality and invoking (57), one finds

$$\begin{aligned}
-\log \int_{\Omega} \frac{\mathcal{I}_h(e^{(1+\delta)v_h^{n+1}(\mathbf{x})})}{\|u_h^0\|_{L^1(\Omega)}} d\mathbf{x} &= -\log \sum_{\mathbf{a} \in \mathcal{N}_h} \frac{e^{(1+\delta)v_h^{n+1}(\mathbf{a})}}{u_h^{n+1}(\mathbf{a})} \frac{u_h^{n+1}(\mathbf{a})}{\|u_h^0\|_{L^1(\Omega)}} \int_{\Omega} \varphi_{\mathbf{a}}(\mathbf{x}) d\mathbf{x} \\
&\leq \sum_{\mathbf{a} \in \mathcal{N}_h} -\log \left(\frac{e^{(1+\delta)v_h^{n+1}(\mathbf{a})}}{u_h^{n+1}(\mathbf{a})} \right) \frac{u_h^{n+1}(\mathbf{a})}{\|u_h^0\|_{L^1(\Omega)}} \int_{\Omega} \varphi_{\mathbf{a}}(\mathbf{x}) d\mathbf{x} \\
&= -\frac{1+\delta}{\|u_h^0\|_{L^1(\Omega)}} (u_h^{n+1}, v_h^{n+1})_h \\
&\quad + \frac{1}{\|u_h^0\|_{L^1(\Omega)}} (\log u_h^{n+1}, u_h^{n+1})_h
\end{aligned}$$

and hence

$$\begin{aligned}
-(u_h^{n+1}, v_h^{n+1})_h + (\log u_h^{n+1}, u_h^{n+1})_h &\geq \delta(u_h^{n+1}, v_h^{n+1})_h + \|u_h^0\|_{L^1(\Omega)} \log \|u_h^0\|_{L^1(\Omega)} \\
&\quad - \|u_h^0\|_{L^1(\Omega)} \log \int_{\Omega} \mathcal{I}_h(e^{(1+\delta)v_h^{n+1}(\mathbf{x})}) d\mathbf{x}.
\end{aligned}$$

In virtue of (18), we can bound

$$\begin{aligned}
\log \int_{\Omega} \mathcal{I}_h(e^{(1+\delta)v_h^{n+1}(\mathbf{x})}) d\mathbf{x} &\leq \log \left(C_{\Omega} (1 + C_{\text{MT}}(1 + \delta)^2 \|\nabla v_h^{n+1}\|^2) \right) \\
&\quad + \frac{(1 + \delta)^2}{8\theta_{\Omega}} \|\nabla v_h^{n+1}\|^2 + \frac{1 + \delta}{|\Omega|} \|v_h^{n+1}\|_{L^1(\Omega)} \\
&= \log \left(\frac{C_{\Omega}}{\varepsilon} \right) + \log \left(\varepsilon (1 + C_{\text{MT}}(1 + \delta)^2 \|\nabla v_h^{n+1}\|^2) \right) \\
&\quad + \frac{(1 + \delta)^2}{8\theta_{\Omega}} \|\nabla v_h^{n+1}\|^2 + \frac{1 + \delta}{|\Omega|} \|v_h^{n+1}\|_{L^1(\Omega)} \\
&\leq \frac{C_{\Omega}}{\varepsilon} + \varepsilon + C_{\text{MT}} \varepsilon (1 + \delta)^2 \|\nabla u_h^{n+1}\|^2 \\
&\quad + \frac{(1 + \delta)^2}{8\theta_{\Omega}} \|\nabla v_h^{n+1}\|^2 + \frac{1 + \delta}{|\Omega|} \|v_h^{n+1}\|_{L^1(\Omega)}.
\end{aligned}$$

Therefore,

$$\begin{aligned}
-(u_h^{n+1}, v_h^{n+1})_h + (\log u_h^{n+1}, u_h^{n+1})_h &\geq \delta(u_h^{n+1}, v_h^{n+1})_h + \|u_h^0\|_{L^1(\Omega)} \log \|u_h^0\|_{L^1(\Omega)} \\
&\quad - \|u_h^0\|_{L^1(\Omega)} \left(\frac{C_{\Omega}}{\varepsilon} + \varepsilon \right) \\
&\quad - C_{\text{MT}} \varepsilon (1 + \delta)^2 \|u_h^0\|_{L^1(\Omega)} \|\nabla v_h^{n+1}\|^2 \\
&\quad - \frac{(1 + \delta)^2 \|u_h^0\|_{L^1(\Omega)}}{8\theta_{\Omega}} \|\nabla v_h^{n+1}\|^2 \\
&\quad - \frac{(1 + \delta) \|u_h^0\|_{L^1(\Omega)}}{|\Omega|} \|v_h^{n+1}\|_{L^1(\Omega)}.
\end{aligned}$$

On recalling (36) and on noting (69), it follows from $x \log x > -\frac{1}{e}$ for $x > 0$ that

$$\begin{aligned}
\mathcal{E}_0(u_h^{n+1}, v_h^{n+1}) &\geq \frac{1}{2} \|v_h^{n+1}\|_h^2 + \frac{1}{2} \|\nabla v_h^{n+1}\|^2 + \delta(u_h^{n+1}, v_h^{n+1})_h \\
&\quad + \|u_h^0\|_{L^1(\Omega)} \left(\log \|u_h^0\|_{L^1(\Omega)} - \frac{C_{\Omega}}{\varepsilon} - \varepsilon \right) \\
&\quad - \frac{(1 + \delta)^2 [8\theta_{\Omega} C_{\text{MT}} \varepsilon + 1] \|u_0\|_{L^1(\Omega)}}{8\theta_{\Omega}} \|\nabla v_h^{n+1}\|^2 \\
&\quad - \frac{(1 + \delta) \|u_h^0\|_{L^1(\Omega)}}{|\Omega|} \|v_h^{n+1}\|_{L^1(\Omega)} \\
&\geq \frac{1}{2} \|v_h^{n+1}\|_h^2 + \delta(u_h^{n+1}, v_h^{n+1})_h - \frac{1}{e} \\
&\quad - \|u_h^0\|_{L^1(\Omega)} \left(\frac{C_{\Omega}}{\varepsilon} + \varepsilon + \frac{(1 + \delta)}{|\Omega|} \|v_h^{n+1}\|_{L^1(\Omega)} \right).
\end{aligned}$$

Finally, we have, from (58), that

$$\begin{aligned} \delta(u_h^{n+1}, v_h^{n+1})_h &\leq \mathcal{E}_0(u_h^{n+1}, v_h^{n+1}) + \frac{1}{e} \\ &\quad + \|u_h^0\|_{L^1(\Omega)} \left(\frac{C_\Omega}{\varepsilon} + \varepsilon + \frac{(1+\delta)}{|\Omega|} (\|v_h^0\|_{L^1(\Omega)} + \|u_h^0\|_{L^1(\Omega)}) \right); \end{aligned}$$

thus, proving the result. \square

The following is an immediate consequence of Lemma 4.5.

Corollary 4.6 (Control of $\|u_h^{n+1} \log u_h^{n+1}\|_{L^1(\Omega)}$). *Under the conditions of Lemma 4.1, there holds*

$$(70) \quad \|u_h^{n+1} \log u_h^{n+1}\|_{L^1(\Omega)} \leq (1 + \frac{1}{\delta}) \mathcal{E}_0(u_h^{n+1}, v_h^{n+1}) + \mathcal{R}_0^{\varepsilon, \delta}(u_h^0, v_h^0) + 2 \frac{|\Omega|}{e}.$$

Proof. Write

$$(71) \quad \begin{aligned} \|u_h^{n+1} \log u_h^{n+1}\|_{L^1(\Omega)} &= - \int_{\Omega} u_h^{n+1}(\mathbf{x}) \log_- u^{n+1}(\mathbf{x}) \, d\mathbf{x} \\ &\quad + \int_{\Omega} u_h^{n+1}(\mathbf{x}) \log_+ u^{n+1}(\mathbf{x}) \, d\mathbf{x}. \end{aligned}$$

Clearly, from $-\frac{1}{e} \leq x \log x \leq 0$ for $x \in [0, 1]$, one gets

$$(72) \quad - \int_{\Omega} u_h^{n+1}(\mathbf{x}) \log_- u^{n+1}(\mathbf{x}) \, d\mathbf{x} \leq \frac{|\Omega|}{e}.$$

By the definition of $\mathcal{E}_0(u_h^{n+1}, v_h^{n+1})$, one can easily deduce from (68) that

$$(73) \quad \begin{aligned} \int_{\Omega} u_h^{n+1}(\mathbf{x}) \log_+ u^{n+1}(\mathbf{x}) \, d\mathbf{x} &\leq \mathcal{E}_0(u_h^{n+1}, v_h^{n+1}) - \int_{\Omega} u_h^{n+1}(\mathbf{x}) \log_- u^{n+1}(\mathbf{x}) \, d\mathbf{x} \\ &\quad + (u_h^{n+1}, v_h^{n+1})_h \\ &\leq (1 + \frac{1}{\delta}) \mathcal{E}_0(u_h^{n+1}, v_h^{n+1}) + \mathcal{R}_0^{\varepsilon, \delta}(u_h^0, v_h^0) + \frac{|\Omega|}{e}. \end{aligned}$$

Thus, inserting (72) and (73) into (71) yields (70). \square

At this point a local-in-time, *a priori* bound for u_h^{n+1} and v_h^{n+1} on which an induction procedure will be applied is derived.

Lemma 4.7 (*A priori* bounds). *Suppose that the conditions of Lemma 4.1 are fulfilled. Let $(u_h^{n+1}, v_h^{n+1}) \in X_h^2$ be the discrete solution computed via (32) and (33). Then there holds*

$$(74) \quad \begin{aligned} &\mathcal{E}_1(u_h^{n+1}, v_h^{n+1}) - \mathcal{E}_1(u_h^n, v_h^n) + 2k\|\tilde{\Delta}_h v_h^{n+1}\|^2 \\ &\quad + k(\mathcal{R}_1^{\gamma, h}(u_h^{n+1}, v_h^{n+1})\|\nabla u_h^{n+1}\|^2 + \frac{1}{2}\|\nabla \tilde{\Delta}_h v_h^{n+1}\|^2) \\ &\leq Ck \left(\|\delta_t v_h^{n+1}\|_h + \|\delta_t v_h^{n+1}\|_h^2 \right) \|u_h^{n+1}\|_h^2 \\ &\quad + Ck\|u_h^{n+1} \log u_h^{n+1}\|_{L^1(\Omega)} + Ck\|u_h^0\|_{L^1(\Omega)}, \end{aligned}$$

where $\mathcal{E}_1(\cdot, \cdot)$ is defined in (37) and

$$\mathcal{R}_1^{\gamma, h}(u_h^{n+1}, v_h^{n+1}) := \frac{4}{3} - \gamma - \gamma^3 \|u_h^{n+1} \log u_h^{n+1}\|_{L^1(\Omega)} - Ch^{1-\frac{2}{p}} \mathcal{F}(u_h^0, v_h^0).$$

Proof. Set $x_h = u_h^{n+1}$ in (32) to obtain

$$(75) \quad \|u_h^{n+1}\|_h^2 - \|u_h^n\|_h^2 + \|u_h^{n+1} - u_h^n\|_h^2 + 2k\|\nabla u_h^{n+1}\|^2 = 2k(\nabla v_h^n, \bar{u}_h^{n+1} \nabla u_h^{n+1}).$$

Consider $T \in \mathcal{T}_h$ and let \mathbf{b}_T be its barycenter to write

$$u_h^{n+1}(\mathbf{b}_T) = u_h^{n+1}(\mathbf{a}_{\bar{u}^i}^T) + \nabla u_h^{n+1}|_T \cdot (\mathbf{b}_T - \mathbf{a}_{\bar{u}^i}^T)$$

and

$$u_h^{n+1}(\mathbf{b}_T) = u_h^{n+1}(\mathbf{a}_{\underline{u}^i}^T) + \nabla u_h^{n+1}|_T \cdot (\mathbf{b}_T - \mathbf{a}_{\underline{u}^i}^T);$$

thereby,

$$(76) \quad u_h^{n+1}(\mathbf{b}_T) = \frac{1}{2}(u_h^{n+1}(\mathbf{a}_{\bar{u}^i}^T) + u_h^{n+1}(\mathbf{a}_{\underline{u}^i}^T)) + \frac{1}{2}\nabla u_h^{n+1}|_T \cdot ((\mathbf{b}^T - \mathbf{a}_{\bar{u}^i}^T) + (\mathbf{b}^T - \mathbf{a}_{\underline{u}^i}^T)).$$

To deal with the right-hand side of (75), we proceed as follows. Let us write

$$(77) \quad (\nabla v_h^n, \bar{u}_h^{n+1} \nabla u_h^{n+1}) = \sum_{i=1}^2 \sum_{T \in \mathcal{T}_h} \int_T \partial_{\mathbf{x}_i} v_h^n u_h^{n+1}(\mathbf{b}_T) \partial_{\mathbf{x}_i} u_h^{n+1} \, d\mathbf{x}.$$

Thus, on substituting (76) into (77), we arrive at

$$\begin{aligned} \int_T \partial_{\mathbf{x}_i} v_h^n u_h^{n+1}(\mathbf{b}_T) \partial_{\mathbf{x}_i} u_h^{n+1} \, d\mathbf{x} &= \int_T \partial_{\mathbf{x}_i} v_h^n u_h^{n+1}(\mathbf{b}_T) \frac{u_h^{n+1}(\mathbf{a}_{\bar{u}^i}^T) - u_h^{n+1}(\mathbf{a}_{\underline{u}^i}^T)}{(\mathbf{a}_{\bar{u}^i}^T - \mathbf{a}_{\underline{u}^i}^T)_i} \, d\mathbf{x} \\ &= \frac{1}{2} \int_T \partial_{\mathbf{x}_i} v_h^n (u_h^{n+1}(\mathbf{a}_{\bar{u}^i}^T) + u_h^{n+1}(\mathbf{a}_{\underline{u}^i}^T)) \frac{u_h^{n+1}(\mathbf{a}_{\bar{u}^i}^T) - u_h^{n+1}(\mathbf{a}_{\underline{u}^i}^T)}{(\mathbf{a}_{\bar{u}^i}^T - \mathbf{a}_{\underline{u}^i}^T)_i} \, d\mathbf{x} \\ &\quad + \int_T \partial_{\mathbf{x}_i} v_h^n \nabla u_h^{n+1} \cdot ((\mathbf{b}_T - \mathbf{a}_{\bar{u}^i}^T) + (\mathbf{b}_T - \mathbf{a}_{\underline{u}^i}^T)) \partial_{\mathbf{x}_i} u_h^{n+1} \, d\mathbf{x} \\ &= \frac{1}{2} \int_T \partial_{\mathbf{x}_i} v_h^n \partial_{\mathbf{x}_i} \mathcal{I}_h(u_h^{n+1})^2 \, d\mathbf{x} \\ &\quad + \int_T \partial_{\mathbf{x}_i} v_h^n \nabla u_h^{n+1} \cdot ((\mathbf{b}_T - \mathbf{a}_{\bar{u}^i}^T) + (\mathbf{b}_T - \mathbf{a}_{\underline{u}^i}^T)) \partial_{\mathbf{x}_i} u_h^{n+1} \, d\mathbf{x}, \end{aligned}$$

which combined with (77) shows that

$$\begin{aligned} (\nabla v_h^n, \bar{u}_h^{n+1} \nabla u_h^{n+1}) &= \frac{1}{2}(\nabla v_h^{n+1}, \nabla \mathcal{I}_h(u_h^{n+1})^2) \\ &\quad + \frac{1}{2}(\nabla(v_h^n - v_h^{n+1}), \nabla \mathcal{I}_h(u_h^{n+1})^2) \\ (78) \quad &\quad + \sum_{i=1}^2 \sum_{T \in \mathcal{T}_h} \int_T \partial_{\mathbf{x}_i} v_h^n \nabla u_h^{n+1} \cdot (\mathbf{b}_T - \mathbf{a}_{\bar{u}^i}^T) \partial_{\mathbf{x}_i} u_h^{n+1} \, d\mathbf{x} \\ &\quad + \sum_{i=1}^2 \sum_{T \in \mathcal{T}_h} \int_T \partial_{\mathbf{x}_i} v_h^n \nabla u_h^{n+1} \cdot (\mathbf{b}_T - \mathbf{a}_{\underline{u}^i}^T) \partial_{\mathbf{x}_i} u_h^{n+1} \, d\mathbf{x} \\ &:= I_1 + I_2 + I_3 + I_4. \end{aligned}$$

It remains to bound each term of (78). We first proceed with I_1 . Choose $x_h = \frac{1}{2}\mathcal{I}_h(u_h^{n+1})^2$ in (33) to write

$$\begin{aligned} I_1 &= -\frac{1}{2}(\delta_t v_h^{n+1}, \mathcal{I}_h(u_h^{n+1})^2)_h - \frac{1}{2}(v_h^{n+1}, \mathcal{I}_h(u_h^{n+1})^2)_h + \frac{1}{2}(u_h^{n+1}, \mathcal{I}_h(u_h^{n+1})^2)_h \\ &:= J_1 + J_2 + J_3. \end{aligned}$$

An estimate for J_1 is easily computed from (16) for $n = 2, 4$ and the Gagliardo-Nirenberg interpolation $\|x_h\|_{L^4(\Omega)} \leq C\|x_h\|^{\frac{1}{2}}\|x_h\|_{H^1(\Omega)}^{\frac{1}{2}}$. It is given by

$$\begin{aligned} J_1 &\leq C\|\delta_t v_h^{n+1}\|_h \|u_h^{n+1}\|_{L^4(\Omega)}^2 \\ &\leq C\|\delta_t v_h^{n+1}\|_h (\|\nabla u_h^{n+1}\| \|u_h^{n+1}\|_h + \|u_h^{n+1}\|_h^2) \\ &\leq C(\|\delta_t v_h^{n+1}\|_h + \|\delta_t v_h^{n+1}\|_h^2) \|u_h^{n+1}\|_h^2 + \frac{\gamma}{4} \|\nabla u_h^{n+1}\|^2 \end{aligned}$$

where $\gamma > 0$ is a constant to be adjusted later on. From (49) and (50), we know that $J_2 \leq 0$. For J_3 , we use the interpolation $\|x_h\|_{L^3(\Omega)} \leq \tilde{\gamma} \|\nabla x_h\|^{\frac{2}{3}} \|x_h \log |x_h|\|_{L^1(\Omega)}^{\frac{1}{3}} + C_{\tilde{\gamma}} \|x_h \log |x_h|\|_{L^1(\Omega)} + C_{\tilde{\gamma}} \|x_h\|_{L^1(\Omega)}^{\frac{1}{3}}$

for $\tilde{\gamma} > 0$ (see [19, Lemma 3.5]) and (16) for $n = 3$ to obtain

$$\begin{aligned} J_3 &\leq C\|u_h^{n+1}\|_{L^3(\Omega)}^3 \\ &\leq \frac{\gamma^3}{2}\|u_h^{n+1} \log u_h^{n+1}\|_{L^1(\Omega)}\|\nabla u_h^{n+1}\|^2 \\ &\quad + C\|u_h^{n+1} \log u_h^{n+1}\|_{L^1(\Omega)}^3 + C\|u_h^{n+1}\|_{L^1(\Omega)}. \end{aligned}$$

Inequality (9) for $p = 2$ shows that

$$\begin{aligned} I_2 &= -\frac{k}{2}(\nabla \delta_t v_h^{n+1}, \nabla \mathcal{I}_h(u_h^{n+1})^2) \\ &\leq C \frac{k}{h^2} \|\delta_t v_h^{n+1}\|_h \|u_h^{n+1}\|_{L^4(\Omega)}^2 \\ &\leq C \frac{k}{h^2} (\|\delta_t v_h^{n+1}\|_h + \|\delta_t v_h^{n+1}\|_h^2) \|u_h^{n+1}\|_h^2 + \frac{\gamma}{4} \|\nabla u_h^{n+1}\|^2. \end{aligned}$$

We treat I_3 and I_4 together. Thus,

$$\begin{aligned} I_3 + I_4 &\leq Ch \|\nabla v_h^n\|_{L^\infty(\Omega)} \|\nabla u_h^{n+1}\|^2 \leq Ch^{1-\frac{2}{p}} \|\nabla v_h^n\|_{L^p(\Omega)} \|\nabla u_h^{n+1}\|^2 \\ &\leq Ch^{1-\frac{2}{p}} \|\tilde{\Delta}_h v_h^n\| \|\nabla u_h^{n+1}\|^2 \leq Ch^{1-\frac{2}{p}} \mathcal{F}(u_h^0, v_h^0) \|\nabla u_h^{n+1}\|^2. \end{aligned}$$

In the above we used (11), (27), and (48). The estimates for the I_i 's applied to (75) lead to

$$\begin{aligned} \|u_h^{n+1}\|_h^2 &= \|u_h^n\|_h^2 + \|u_h^{n+1} - u_h^n\|_h^2 + 2k\|\nabla u_h^{n+1}\|^2 \\ (79) \quad &\leq C\left(1 + \frac{k}{h^2}\right)k(\|\delta_t v_h^{n+1}\|_h + \|\delta_t v_h^{n+1}\|_h^2) \|u_h^{n+1}\|_h^2 \\ &\quad + k\left(\gamma + \gamma^3\|u_h^{n+1} \log u_h^{n+1}\|_{L^1(\Omega)} + Ch^{1-\frac{2}{p}} \mathcal{F}(u_h^0, v_h^0)\right) \|\nabla u_h^{n+1}\|^2 \\ &\quad + Ck\|u_h^{n+1} \log u_h^{n+1}\|_{L^1(\Omega)}^3 + Ck\|u_h^{n+1}\|_{L^1(\Omega)}. \end{aligned}$$

Choose $x_h = -\tilde{\Delta}^2 v_h^{n+1}$ in (33) to get

$$\begin{aligned} (80) \quad &\|\tilde{\Delta}_h v_h^{n+1}\|_h^2 - \|\tilde{\Delta}_h v_h^n\|_h^2 + \|\tilde{\Delta}_h(v_h^{n+1} - v_h^n)\|_h^2 \\ &\quad + 2k\|\nabla \tilde{\Delta}_h v_h^{n+1}\|_h^2 + 2k\|\tilde{\Delta}_h v_h^{n+1} v_h^{n+1}\|_h^2 = 2k(\nabla u_h^{n+1}, \nabla \tilde{\Delta}_h v_h^{n+1}) \\ &\leq k\left(\frac{4}{3}\|\nabla u_h^{n+1}\|^2 + \frac{3}{2}\|\nabla \tilde{\Delta}_h v_h^{n+1}\|^2\right). \end{aligned}$$

The proof follows by use of (79) and (80). \square

4.3. Induction argument. The essential step to finishing up the proof of Theorem 3.1 is an induction argument on n . We need to verify that the overall sequence $\{u_h^m\}_{m=0}^N$ provided by system (32)-(33) accomplishes the estimates from Theorem 3.1.

Observe first that $\mathcal{F}(u_h^0, v_h^0)$ is uniformly bounded with regard to h , because of (29) and (31), and hence we are allowed to choose (h, k) satisfying (39) and (40).

• **Case ($m = 1$).** We want to prove Theorem 3.1 for $m = 1$. Inequality (48) holds trivially, since $\mathcal{F}(u_h^0, v_h^0)$ is bounded independently of (h, k) ; thereby, from (49) and (50), we obtain, for $n = 0$, that, for all $\mathbf{x} \in \Omega$,

$$(81) \quad u_h^1(\mathbf{x}) > 0$$

and

$$(82) \quad u_h^1(\mathbf{x}) \geq 0.$$

Likewise, we have, by (57) and (58) for $n = 0$, that

$$\|u_h^1\|_{L^1(\Omega)} = \|u_h^0\|_{L^1(\Omega)}$$

and

$$\|v_h^1\|_{L^1(\Omega)} \leq \|v_h^0\|_{L^1(\Omega)} + \|u_h^0\|_{L^1(\Omega)}.$$

In view of (81) and (82), inequality (62) for $n = 0$ shows that

$$\begin{aligned} &\mathcal{E}_0(u_h^1, v_h^1) - \mathcal{E}_0(u_h^0, v_h^0) + k\|\delta_t v_h^1\|_h^2 \\ &\quad + k\|\mathcal{A}_h^{-\frac{1}{2}}(u_h^1) \nabla u_h^1 - \mathcal{A}_h^{\frac{1}{2}}(u_h^1) \nabla v_h^0\|^2 \leq 0 \end{aligned}$$

which, in turn, gives

$$(83) \quad \mathcal{E}_0(u_h^1, v_h^1) \leq \mathcal{E}_0(u_h^0, v_h^0).$$

Applying (83) to (68) and (70) for $n = 0$ yields that

$$(84) \quad \begin{aligned} (u_h^1, v_h^1)_h &\leq \frac{1}{\delta} \mathcal{E}_0(u_h^0, v_h^0) + \mathcal{R}_0^{\delta, \varepsilon}(u_h^0, v_h^0) \\ &:= \mathcal{B}_0(u_h^0, v_h^0), \end{aligned}$$

and

$$(85) \quad \begin{aligned} \|u_h^1 \log u_h^1\|_{L^1(\Omega)} &\leq (1 + \frac{1}{\delta}) \mathcal{E}_0(u_h^0, v_h^0) + \mathcal{R}_0^{\varepsilon, \delta}(u_h^0, v_h^0) + 2 \frac{|\Omega|}{e} \\ &:= \mathcal{B}_1(u_h^0, v_h^0). \end{aligned}$$

As a result of applying (84) and (85) to (62) for $n = 0$, we find

$$\begin{aligned} k \|\delta_t v_h^1\|_h^2 &\leq \mathcal{E}_0(u_h^0, v_h^0) - \mathcal{E}_0(u_h^1, v_h^1)_h \\ &\leq \mathcal{E}_0(u_h^0, v_h^0) + \mathcal{B}_0(u_h^0, v_h^0) + \mathcal{B}_1(u_h^0, v_h^0) \\ &:= \mathcal{B}_2(u_h^0, v_h^0). \end{aligned}$$

Selecting γ to be sufficiently small such that

$$(86) \quad \gamma + \gamma^3 \mathcal{B}_2(u_h^0, v_h^0) \leq \frac{5}{12}$$

and recalling (46), this implies, from (83), that

$$\mathcal{R}_1^{\gamma, h}(u_h^1, v_h^1) \geq \frac{4}{3} - \gamma - \gamma^3 \mathcal{B}_2(u_h^0, v_h^0) - Ch^{1-\frac{1}{p}} \mathcal{E}_1(u_h^0, v_h^0) \geq \frac{1}{2};$$

thus, one can find upon using (74) for $n = 0$ that

$$(87) \quad \begin{aligned} \mathcal{E}_1(u_h^1, v_h^1) - \mathcal{E}_1(u_h^0, v_h^0) + 2k \|\tilde{\Delta}_h v_h^1\|^2 + \frac{k}{2} (\|\nabla u_h^1\|^2 + \|\nabla \tilde{\Delta}_h v_h^1\|^2) \\ \leq Ck (\|\delta_t v_h^1\|_h + \|\delta_t v_h^1\|_h^2) \|u_h^1\|^2 + Ck \mathcal{B}_1^3(u_h^0, v_h^0) + Ck \|u_h^0\|_{L^1(\Omega)}. \end{aligned}$$

Grönwall's inequality now provides the bound

$$\mathcal{E}_1(u_h^1, v_h^1) + \frac{k}{2} (\|\nabla u_h^1\|^2 + \|\nabla \tilde{\Delta}_h v_h^1\|^2) \leq \mathcal{F}(u_h^0, v_h^0).$$

Theorem 3.1 is therefore verified for $m = 1$.

• **Case $m = n + 1$.** Assume that the bounds in Theorem 3.1 are valid for all $m \in \{1, \dots, n\}$. Consequently, it follows that

$$(88) \quad \begin{aligned} \mathcal{E}_1(u_h^n, v_h^n) + \frac{k}{2} \sum_{r=1}^n (\|\nabla u_h^r\|^2 + \|\nabla \tilde{\Delta}_h v_h^r\|^2) \\ \leq \mathcal{E}_1(u_h^0, v_h^0) + C k \sum_{r=1}^n \left(\|\delta_t v_h^r\|_h + \|\delta_t v_h^r\|_h^2 \right) \|u_h^r\|^2 \\ + C k \sum_{r=1}^n \left(\mathcal{B}_1^3(u_h^0, v_h^0) + \|u_h^0\|_{L^1(\Omega)} \right) \end{aligned}$$

holds on the basis of

$$\mathcal{R}_1^{\gamma, h}(u_h^m, v_h^m) \geq \frac{1}{2} \quad \text{for all } m \in \{0, \dots, n\}.$$

Then we want to prove Theorem 3.1 for $m = n + 1$. Indeed, by the induction hypothesis (47) for $m = n$, it is clear that (48) holds; therefore, one has (49) and (50). That inequalities (43) and (44) are satisfied for $m = n + 1$ is simply by noting (57) and (58). Combining (62) and the induction hypothesis (45) for $m = n$, we deduce (45) for $m = n + 1$, which implies

$$(89) \quad \max_{m \in \{0, \dots, n+1\}} \mathcal{E}_0(u_h^m, v_h^m) \leq \mathcal{E}_0(u_h^0, v_h^0).$$

As a result of this, we have, by (68) and (70), that

$$(90) \quad (u_h^{n+1}, v_h^{n+1})_h \leq \mathcal{B}_0(u_h^0, v_h^0)$$

and

$$(91) \quad \|u_h^{n+1} \log u_h^{n+1}\|_{L^1(\Omega)} \leq \mathcal{B}_1(u_h^0, v_h^0).$$

Moreover, it follows from (45) for $m = n + 1$ that

$$(92) \quad k \sum_{r=0}^{n+1} \|\delta_t v_h^r\|_h^2 \leq \mathcal{B}_2(u_h^0, v_h^0),$$

in view of (90) and (91).

Once again if γ is chosen to be small enough such that (86) holds and condition (46) is invoked, one finds

$$\mathcal{R}_1^{\gamma, h}(u_h^{n+1}, v_h^{n+1}) \geq \frac{4}{3} - \gamma - \gamma^3 \mathcal{B}_2(u_h^0, v_h^0) - Ch^{1-\frac{1}{p}} \mathcal{E}_1(u_h^0, v_h^0) \geq \frac{1}{2}$$

owing to (89). We thus infer from (74) combined with (88) that

$$\begin{aligned} & \mathcal{E}_1(u_h^{n+1}, v_h^{n+1}) + \frac{k}{2} \sum_{r=1}^{n+1} (\|\nabla u_h^r\|^2 + \|\nabla \tilde{\Delta}_h v_h^r\|^2) \\ & \leq \mathcal{E}_1(u_h^0, v_h^0) + C k \sum_{r=1}^{n+1} (\|\delta_t v_h^r\|_h + \|\delta_t v_h^r\|_h^2) \|u_h^r\|^2 \\ & \quad + C k \sum_{r=1}^{n+1} \left(\mathcal{B}_1^3(u_h^0, v_h^0) + C k \|u_h^r\|_{L^1(\Omega)} \right) \end{aligned}$$

and hence Grönwall's inequality provides (47) for $m = n + 1$ when used (92).

5. COMPUTATIONAL EXPERIMENTS

The computational experiments are meant to support and complement the theoretical results in the earlier sections in two different settings. On the one hand, we regard initial data u_0 under the condition $\int_{\Omega} u_0(\mathbf{x}) d\mathbf{x} \in (0, 4\pi)$, which give solutions remaining bounded over time. On the other hand, we use a particularly demanding test where a finite time blowup is expected. For this latter numerical test, it must be said that the blowup setting is out of reach from our analysis since (47) is not satisfied for blowup solutions; therefore, lower bounds cannot be guaranteed. Nevertheless, the results are striking with regard to lower bounds since they fail very close to the expecting blowup time for not so small discrete parameters.

All the computations were performed with the help of the FreeFem++ framework [11].

5.1. Non-blowup setting. As the domain we take the square $\bar{\Omega} = [-1/2, 1/2]^2$. The evolution starts from the bell-shaped initial data

$$(93) \quad u_0 = C_0 e^{-C_0(x^2+y^2)} \quad \text{and} \quad v_0 = C_0 e^{-C_0(x^2+(y-0.5)^2)},$$

which fulfill a homogeneous Neumann boundary condition approximately¹. It should be noticed that u_0 is centered at the origin $(0, 0)$, whereas v_0 is centered at the midpoint of the top edge of the domain. For each C_0 , one can compute that $\int_{\Omega} u_0(\mathbf{x}) d\mathbf{x} \in (0, 4\pi)$; therefore, problem (1) with (2)–(3) has a unique, smooth solution. As a result of this experiment, we expect diffusion and chemotaxis transfer of cells (the u component of the solution) from the center of the domain toward the top edge, where the highest concentration of chemical agent (the v component of the solution) is found.

For the spacial discretization, we introduce the \mathcal{P}_1 finite element space X_h associated with an *acute* mesh \mathcal{T}_h defined as follows. From an $N_{\text{square}} \times N_{\text{square}}$ uniform grid, obtained by dividing Ω into

¹If C_0 is quite small, the Neumann boundary condition on (u_0, v_0) is not approximately null. For this reason, we only take C_0 bigger or equal to 40.

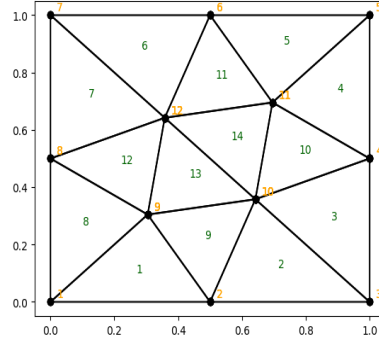
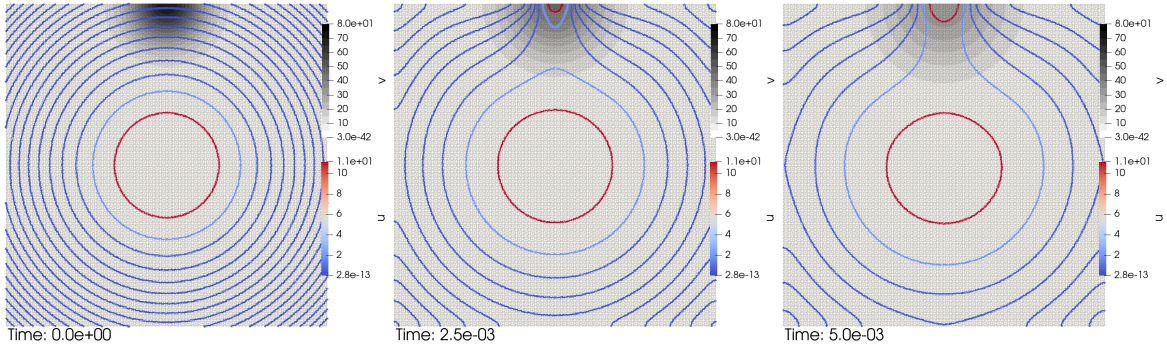


FIGURE 1. Reference macroelement, composed of 14 acute triangles

FIGURE 2. Solution u_h^n (colored isolines) and v_h (gray scale background) at three time steps: $t_n = 0, 2.5 \cdot 10^{-3}$ and $5 \cdot 10^{-3}$. Diffusion and chemotaxis transfer of u_h^n (cells) towards highest concentrations of v_h^n can be seen along time. Acute mesh with $N_{\text{square}} = 50$, $k = 10^{-4}$, initial data parameter: $C_0 = 70$.

macroelements consisting of squares, we construct the mesh \mathcal{T}_h by splitting each macroelement into 14 acute triangles as indicated in Figure 1. This way, for $N_{\text{square}} = 50$, we define a mesh consisting of 35,000 acute triangles and 17,701 vertices with mesh size $h \simeq 0.0101247$. Selecting $C_0 = 70$, we compute $N = 50$ time iterations using scheme (32)–(33) with time step $k = 10^{-4}$. Snapshots of the simulations at times $t_n = 0, 2.5 \cdot 10^{-3}$ and $5 \cdot 10^{-3}$ are collected in Figure 2. The same test is repeated for $C_0 \in \{40, 50, 60\}$, checking that positivity of the numerical solution is preserved over time iterations. In all these cases, the qualitative behavior expected in chemotaxis phenomena is obtained.

Positivity of u_h^{n+1} breaks if C_0 grows beyond $C_0 \simeq 70$, but v_h^{n+1} remains positive. Note that, as C_0 is increased, $\|\nabla v_h^0\|_{L^\infty(\Omega)}$ becomes larger and larger, with v_0 defined in (93); consequently, $\|\nabla v_h^n\|_{L^\infty(\Omega)}$ does at least for the first time steps. Therefore, computing u_h^{n+1} using (32) turns out to be more demanding. Figure 3 (top) plots the values $\{\min_{\mathbf{x} \in \Omega} u_h^n(\mathbf{x}), n = 0, \dots, 50\}$ for $C_0 \in \{70, 80, 90, 100\}$. Positivity is recovered once $\|\nabla v_h^n\|_{L^\infty(\Omega)}$ becomes small enough.

This loss of positivity for large values of C_0 is not in contradiction to (41) in Theorem 3.1, since (39) and (40) are not fulfilled for those cases. Moreover it is remarkable that, for $C_0 \simeq 70$, u_h^{n+1} keeps positivity, even when (39) and (40) are quite far from being verified. In fact, $\mathcal{F}(u_h^0, v_h^0)$ takes huge values, which exceed the capacity of floating point standards. These huge values stem from $\|\nabla v_h^0\| \simeq 7,687.66$, which gives $\mathcal{B}_2(u_h^0, v_h^0) \simeq 23,411.5$, used as an exponent for computing $\mathcal{F}(u_h^0, v_h^0)$. Of course, for small values C_0 , for which condition (39) and (40) are verified, our experiments show

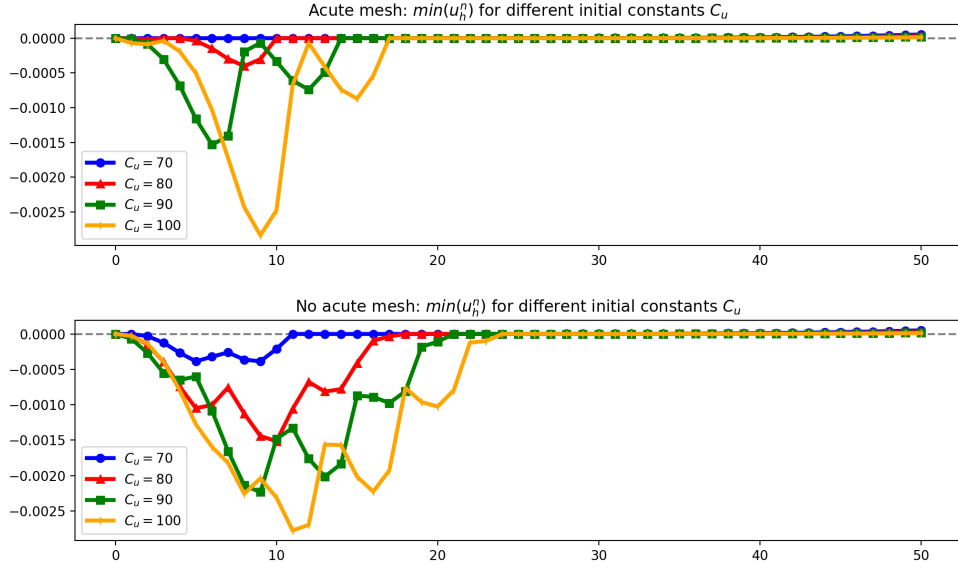


FIGURE 3. Plot of $\min_{\mathcal{T}_h}(u_h^n)$, $n = 0, \dots, 50$, where \mathcal{T}_h is an acute mesh (top) or non-acute mesh (bottom). Initial value constants: $C_0 = 70, 80, 90, 100$.

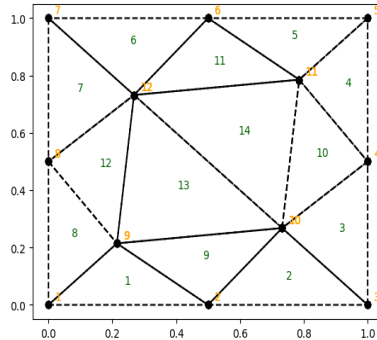


FIGURE 4. Reference macroelement containing some obtuse triangles.

positivity, as expected. In this sense, our numerical experiments suggest that there might be room for improvement in conditions (39) and (40) of Theorem 3.1.

In order to compare the performance of scheme (32)–(33) using a *non-acute* mesh, we consider, as before, a mesh composed of 50×50 macroelements as depicted in Figure 4. This way the theoretical results shown in this paper may not be applied.

Diffusion and chemotaxis movements are obtained as observed in Figure 2 for $C_0 = 70$, but an earlier loss of positivity as well. In particular, it is lost from the first time step ($\min_{\mathcal{T}_h}(u_h^n) \simeq -1.39289 \cdot 10^{-5}$ at $t_n = 10^{-4}$). Positivity is not completely recovered until $t_n = 0.0018$, thereafter positive values persist with time. Figure 3 (bottom) displays the evolution of the values $\{\min_{\mathbf{x} \in \Omega} u_h^n(\mathbf{x}), n = 0, \dots, 50\}$ for $C_0 \in \{70, 80, 90, 100\}$.

5.2. Blowup setting. The second suite of tests is focused on a blowup context. We consider

$$(94) \quad u_0 = C_u e^{-0.1C_u(x^2+y^2)} \quad \text{and} \quad v_0 = C_v e^{-0.1C_v(x^2+y^2)},$$

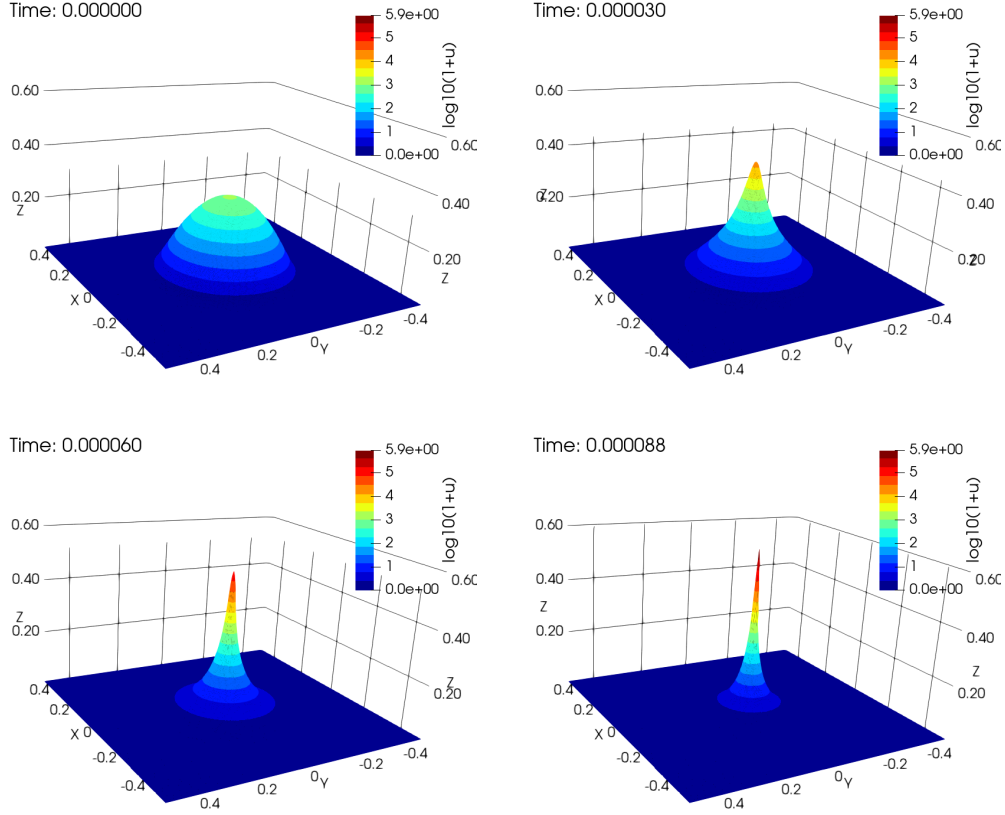


FIGURE 5. Solution u_h^n associated with an acute mesh of 100×100 macroelements at time steps $n = 0, 30, 60$, and 88 (when positivity is broken).

with $C_u = 1000$ and $C_v = 500$. Thus constructed, initial data are large enough to expect a finite time blowup for both u and v components of the continuous solution to problem (1) with (2)–(3). For details, see e.g. [4], where the blowup time t^* is conjectured to be located in the time interval $(4.4 \cdot 10^{-5}, 10^{-4})$.

When used a *acute* mesh of macroelements as in Figure 1 for approximating such a demanding blowup test, scheme (32)–(33) cannot aspire to achieve positivity over the whole blowup interval. The reason is that conditions (39) and (40) in Theorem 3.1 are not fulfilled, because $\|u_h^0\|$ and $\|\nabla v_h^0\|$ are too large ($\|u_h^0\|_h^2 = 15,708$ and $\|\nabla v_h^0\|_{L^2(\Omega)}^2 = 785,230$). However, as in the previous experiments, one does not need (39) and (40) to hold so as to keep positivity. For instance, a value $N_{\text{square}} = 600$ suffices to obtain positivity for the overall blowup interval. Moreover, a value $N_{\text{square}} = 100$ ($h \simeq 0.005$) maintains positivity well into $(4.4 \cdot 10^{-5}, 10^{-4})$. To be more precise, if \mathcal{T}_h is defined by 100×100 macroelements and $k = 10^{-6}$, then $u_h^n > 0$ and $v_h^n > 0$ for $t_n \in [0, 8.7 \cdot 10^{-5}]$. For $t_n = 8.7 \cdot 10^{-5}$ ($n = 88$), one gets $\min_{\mathcal{T}_h}(u_h^n) = -90.7418$. The evolution of u_h^n is shown (on a logarithmic scale) in Figure 5 for time steps $n = 0, 30, 60$, and 88 . A blowup phenomenon in the center of the domain can be observed: the maximum value of u_h^n grows over time, reaching $\max(u_h^n) = 8.85515 \times 10^5$, while its support shrinks.

When considering a *non-acute* mesh of 100×100 macroelements (see Figure 4), we encounter that positivity is only maintained until $t_n = 6.7 \cdot 10^{-5}$. At time $t_n = 6.8 \cdot 10^{-5}$ ($n = 68$), $\min_{\mathcal{T}_h}(u_h^n) = -64.2157$ and $\max_{\mathcal{T}_h}(u_h^n) = 2.16982 \times 10^5$. Figure 6 shows the numerical solution u_h^n at $t_n = 6.8 \cdot 10^{-5}$ (left), when positivity is broken for the first time, and at $t_n = 8.7 \cdot 10^{-5}$ (center), when negative values

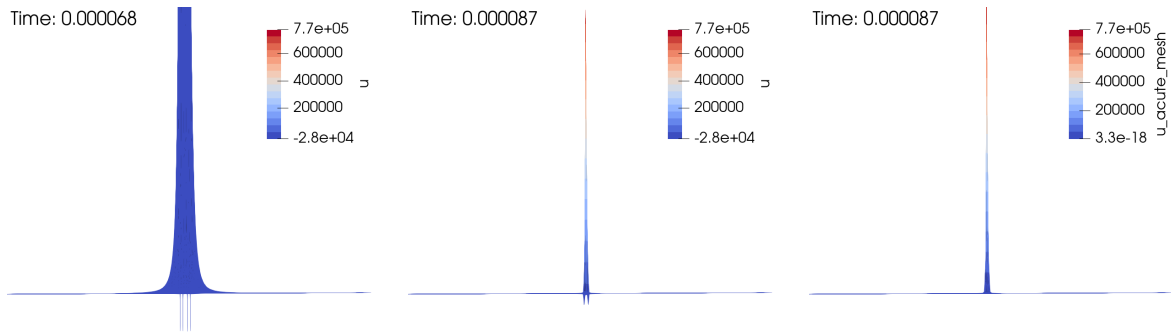


FIGURE 6. Left: zoomed detail of u_h^n associated with a non-acute mesh at $t_n = 6.8 \cdot 10^{-5}$; positivity is broken. Center: u_h^n associated with a non-acute mesh at $t_n = 8.7 \cdot 10^{-5}$; deep negative values appear. Right: u_h^n associated with an acute mesh at $t_n = 8.7 \cdot 10^{-5}$, positivity is maintained.

of order 10^{-4} are reached. Otherwise, the numerical solution u_h^n associated with an acute mesh keeps positivity at time $t_n = 8.7 \cdot 10^{-5}$ (right).

REFERENCES

- [1] BELLOMO, N.; BELLOQUID, A.; TAO, Y.; WINKLER, M., *Toward a mathematical theory of Keller-Segel models of pattern formation in biological tissues*. Math. Models Methods Appl. Sci. 25 (2015), no. 9, 1663–1763.
- [2] BRENNER, S. C.; SCOTT, L. R., *The mathematical theory of finite element methods*. Third edition. Texts in Applied Mathematics, 15. Springer, New York, 2008.
- [3] CHERTOCK, A.; EPSHTEYN, Y.; HU, H.; KURGANOV, A. *High-order positivity-preserving hybrid finite-volume-finite-difference methods for chemotaxis systems*. Adv. Comput. Math. 44 (2018), no. 1, 327–350.
- [4] CHERTOCK, A.; KURGANOV, A. *A second-order positivity preserving central-upwind scheme for chemotaxis and haptotaxis models*. Numer Math, 111 (2008), no. 2, 169–205.
- [5] CHANG, SUN-YUNG A.; YANG, PAUL C., *Conformal deformation of metrics on \mathbb{S}^2* . J. Differential Geom. 27 (1988), no. 2, 259–296.
- [6] DE LEENHEER, P.; GOPALAKRISHNAN, J.; ZUHR, E., *Nonnegativity of exact and numerical solutions of some chemotactic models*. Comput. Math. Appl. 66 (2013), no. 3, 356–375.
- [7] ERN, A.; GUERMOND, J.-L., *Theory and practice of finite elements*. Applied Mathematical Sciences, 159. Springer-Verlag, New York, 2004.
- [8] GIRAUT, V.; LIONS, J.-L., *Two-grid finite-element schemes for the transient Navier-Stokes problem*. M2AN Math. Model. Numer. Anal. 35 (2001), no. 5, 945–980.
- [9] GRISVARD, P., *Elliptic problems in nonsmooth domains*. Monographs and Studies in Mathematics, 24. Pitman (Advanced Publishing Program), Boston, MA, 1985.
- [10] CABRALES, R. C.; GUTIÉRREZ-SANTACREU, J. V.; RODRÍGUEZ-GALVÁN, J. R., *Numerical solution for an aggregation equation with degenerate diffusion*. arXiv:1803.10286.
- [11] HECHT, F., *New development in freefem++*, J. Numer. Math. Vol. 20, No. 3-4 (2012) 251–265.
- [12] HERRERO, M. A.; VELÁZQUEZ, J.J.L., *A blow-up mechanism for a chemotaxis model*, Ann. Scuola Norm. Sup. Pisa Cl. Sci. 24 (1997) 633–683.
- [13] HILLEN, T.; PAINTER, K. J. *A users guide to PDE models for chemotaxis*, J. Math. Biol. 58 (2009) 183–217.
- [14] HORSTMANN, D., *From 1970 until present: the Keller-Segel model in chemotaxis and its consequences. I*. Jahresber. Deutsch. Math.-Verein. 105 (2003), no. 3, 103–165.
- [15] HORSTMANN, D., *From 1970 until present: the Keller-Segel model in chemotaxis and its consequences. II*. Jahresber. Deutsch. Math.-Verein. 106 (2004), no. 2, 51–69.
- [16] HORSTMANN, D.; WANG, G., *Blow-up in a chemotaxis model without symmetry assumptions*, Eur. J. Appl. Math. 12 (2001) 159–177.
- [17] KELLER, E. F.; L. A. SEGEL, *Initiation of slide mold aggregation viewed as an instability*, J. Theor. Biol. 26 (1970) 399–415.
- [18] KELLER; E. F.; L. A. SEGEL, *Model for chemotaxis*, J. Theor. Biol. 30 (1971) 225–234.
- [19] NAGAI, T; SENBA, T; YOSHIDA, K., *Application of the Trudinger-Moser inequality to a parabolic system of chemotaxis*, Funkcial. Ekvac. 40 (1997) 411–433.
- [20] SAITO, N., *Error analysis of a conservative finite-element approximation for the Keller-Segel system of chemotaxis*. Commun. Pure Appl. Anal. 11 (2012), no. 1, 339–364.

- [21] SCOTT, L.R.; ZHANG, S. *Finite element interpolation of non-smooth functions satisfying boundary conditions.* Math. Comp. 54 (1990) 483–493.
- [22] STREHL, R.; SOKOLOV, A.; KUZMIN, D.; TUREK, S., *A flux-corrected finite element method for chemotaxis problems.* Comput. Methods Appl. Math. 10 (2010), no. 2, 219–232.
- [23] SULMAN, M.; NGUYEN, T. *A Positivity Preserving Moving Mesh Finite Element Method for the Keller–Segel Chemotaxis Model* J. Sci. Comp. 80 (2019), no. 1, 649–666.
- [24] WINKLER, M., *Finite-time blow-up in the higher-dimensional parabolic-parabolic Keller-Segel system.* J. Math. Pures Appl. (9) 100 (2013), no. 5, 748–767.
- [25] LI, X. H.; SHU, C.-W.; YANG, Y., *Local discontinuous Galerkin method for the Keller-Segel chemotaxis model.* J. SCI. COMPUT. 73 (2017), NO. 2-3, 943–967.

†DPTO. DE MATEMÁTICA APLICADA I, E. T. S. I. INFORMÁTICA, UNIVERSIDAD DE SEVILLA, AVDA. REINA MERCEDES, S/N., E-41012 SEVILLA, SPAIN, E-MAIL: juanvi@us.es

‡ DEPARTAMENTO DE MATEMÁTICAS. FACULTAD DE CIENCIAS. CAMPUS UNIVERSITARIO DE PUERTO REAL, UNIVERSIDAD DE CÁDIZ. E-11510 PUERTO REAL, CÁDIZ E-MAIL: rafael.rodriguez@uca.es